Electronic Supplementary Material (ESI) for Journal of Materials Chemistry C.
This journal is © The Royal Society of Chemistry 2020

Supporting Information

for

Tunable Ultralong Organic Phosphorescence Modulated by Main-Group Elements with Different Lewis Acidity and Basicity

Letian Xu,‡[ab] Kun Zhou,‡[ab] Xinyu Qiu,[d] Bin Rao,[b] Dandan Pei,*[a] Ang Li,[a] Zhongfu An[c] and Gang He*[ab]

[a]Key Laboratory of Shaanxi Province for Craniofacial Precision Medicine Research College of Stomatology, Xi’an Jiaotong University, Xi’an, Shaanxi province, 710049 (China)

E-mail: ganghe@mail.xjtu.edu.cn (G. He); peidandan1986@126.com (D. Pei)

[b]Frontier Institute of Science and Technology, State Key Laboratory for Strength and Vibration of Mechanical Structures, Xi’an Jiaotong University, Xi’an, Shaanxi province, 710054 (China)

[c]Key Laboratory of Flexible Electronics (KLOFE) & Institute of Advanced Materials (IAM), Nanjing Tech University, Nanjing, Jiangsu province, 211816 (China)

[d]Center for Tissue Engineering, School of Stomatology, Fourth Military Medical University, Xi’an, Shaanxi Province, 710032 (China)

‡ These authors contributed equally to this work.

Contents

1. Materials and instrumentation

General. THF and Toluene were freshly distilled under argon from sodium/benzophenone prior to use. Triphenylmethyl bromide (98%), bis(4-bromophenyl)amine (97%), copper(I) bromide (99%), 4-dimethylaminopyridine (98%), sulfuryl chloride (98%), sodium hydride (60% dispersion in mineral oil), Diphenyl disulfide (98%), benzenesulfonyl chloride (99%), tetrabutylammonium bromide (99%), Ammonium chloride (99%), Sodium chloride (99%), Sodium bicarbonate (99%), carbazole (97%), 1,2-Dichloroethane (99%) Iodobenzene (98%), 2-Bromoaniline (98%), Tris(dibenzylideneacetone)dipalladium (98%), Sodium tert-butoxide (98%), Dioxane (99.7%, Extra Dry), 2-Dicyclohexylphosphino-2'-(N,N-dimethylamino)biphenyl (98%), Potassium carbonate (99%), Palladium diacetate (99%), Tricyclohexylphosphonium tetrafluoroborate (98%), N,N-Dimethylacetamide (99.8%, Extra Dry) were purchased from Energy Chemical Inc. n-Butyllithium (2.5 mol/L in hexane) was purchased from Acros. Dimesitylboron fluoride (98%) was purchased from Aldrich. The carbazole was sysnthsised according to the previously reported literiture.[1, 2] If no other special indicated, other reagents and solvents were used as commercially available without further purification. Column chromatographic purification of products was accomplished using 200-300 mesh silica gel.

NMR spectra were measured on a Bruker Avance-400 spectrometer in the solvents indicated; chemical shifts are reported in units (ppm) by assigning TMS resonance in the ^{1}H spectrum as 0.00 ppm, $CDCl_3$ resonance in the ^{13}C spectrum as 77.0 ppm. Coupling constants are reported in Hz with multiplicities denoted as s (singlet), d (doublet), t (triplet), q (quartet) and m (multiplet). High performance liquid chromatography (HPLC) were measured using Aglient 1260 Infinity II, the isopropanol-hexane ratio is 10/90. UV-vis measurements were performed using DH-2000-BAL Scan spectrophotometer. Steady-state photoluminescence spectra and excitation spectra were measured using Horiba PL spectrometer (Fluorolog-3). Steady-state phosphorescence spectra and excitation spectra were measured using Hitachi F-4600. The photoluminescence quantum efficiency, time-resolved emission spectra and lifetime were obtained using Edinburgh FLSP980 fluorescence spectrophotometer equipped with a xenon lamp (Xe900), a picosecond pulsed laser (EPL-375), a microsecond flash-lamp (μF900) and an integrating sphere, respectively. Single crystal X-ray diffraction analysis was carried out on a Bruker apex duo equipment. Elemental analysis was conducted using a Euro vector EA3000 Analyzer. High-resolution mass spectra (HRMS) were collected on a Bruker maxis UHR-TOF mass spectrometer in an ESI positive mode. Transmission electron microscopy was used to record the TEM images via field emission transmission electron microscope JEOL JEM-F200 (HR). Delsa Nano C was used to measure the diameter of nanocrystals. Afterglow imaging was performed by LVIS SPECTR system. The luminescent photos were taken by a Nikon D5100 camera under the irradiation of hand-held UV lamp at room temperature.

Nanoparticles preparation

The top-down approach to prepare nanoparticles was based on the literature procedure with slight modification.[3-5] Firstly, F127 (PEG-b-PEG-b-PEG, 10 mg) was dissolve in 3 mL deionic water. Then, the **CCz** powder (1 mg) was added into the aqueous solution of F127 under sonication for 15 min. The mixture was filtered by a 0.22 μm syringe driven filter (polyvinylidene fluoride (PVDF) membrane with millipore) to afford water-dispersible nanoparticles.

Cell viability assay

L-929 mouse fibroblast was cultured in dulbecco's modified eagle medium supplemented with 10% FBS at 37 °C in a humified atmosphere containing 5% CO_2. L-929 mouse fibroblast was seeded in 96-well U-bottom plates at a density of 8×10^3 cells/well until adherent. And incubated with different concentration CCz nanoparticles (0.1, 0.2, 0.39, 0.78, 1.56, 3.13, 6.25, 12.5, 25, 50, 100 and 200 μg mL-1) in liquid culture medium at 37 °C for 48 h. Subsequently, MTT (1 mg mL^{-1} in medium, 100 μL/well) was added to the wells after the supernatant was removed followed by incubation at 37 ^{o}C for 48 h. The supernatant was removed and 100 μL DMSO per well was added to dissolve the produced formazan. After shaking the plates for 10 min, absorbance values of the wells were read with a microplate reader at 520 nm. The cell viability rate (VR) was calculated according to the following equation:

$$\mathrm{VR} = \frac{\mathrm{A}}{\mathrm{A_0}} \times 100\%$$

where A is the absorbance of the experimental groups, and the A_0 is the absorbance of the control group.

In vivo UOP imaging

All of the procedures of animal experiments were performed according to the guidelines established by the animal research committee of Xi'an Jiaotong University. The mice were firstly anesthetized using 2% isoflurane in oxygen, which was then subcutaneously treated with **CCz** nanoparticles (0.8 μM) at the left-back. The mice were then placed into the IVIS instrument, exposure to 365 nm UV lamp (15 mW $\mathrm{cm^{-2}}$) for 30 s. Afterward, the images were acquired within 5s at different time points (0,1 h) after removal of the light source using IVIS system under the bioluminescence mode (exposure time: 15 s). During the imaging, the mice were warmed with a heating pad under continued isoflurane anesthesia. Alternatively, the mice were treated **CCz** nanoparticles (0.8 μM) through tail intravenous injection. The **CCz** nanoparticles were activated by 365 nm UV lamp (15 mW $\mathrm{cm^{-2}}$) for 30 s, and then imaged with IVIS system following the same method. In addition, the *in vivo* fluorescence imaging was also performed (Excitation: 430 nm; Emission: 560 nm).

Histological studies

To determine the damage of major organs of mice before and after **CCz** nanoparticles treation, the major organs were imaged by a digital camera. The harvested organs were fixed in 4% phosphate-buffered paraformaldehyde for 12 h and embedded in paraffin. Ten micrometers of thick serial sections were cut from the paraffin-embedded blocks and underwent haemotoxylin and eosin (H&E) staining. The slices were examined under a digital microscope.

Blood chemical analysis

The blood biochemistry analysis (AST, ALT, ALB, CRE, BUN, and TB) was determined by a biochemical analyzer. Triplicate measurements were conducted for the studies.

2. Synthetic procedures

Synthesis of 9-(dimesitylboranyl)-9*H*-carbazole (BCz).

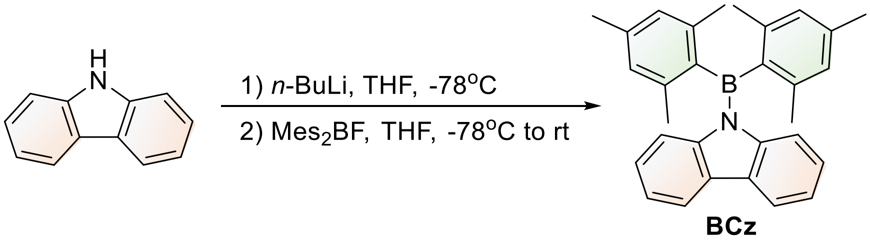

To a solution of carbazole (0.836 g, 5.0 mmol) in THF (40 mL) was added *n*-BuLi (2.50 M in hexane, 2.40 mL, 6 mmol) dropwise at -78 °C. After the reaction mixture was stirred at -78 °C for 30 min, dimesitylfluoroborane (1.475 g, 5.5 mmol) in 10 mL dry THF was added to the mixture at –78 °C. The reaction mixture was gradually warmed to room temperature and then stirred overnight. After the reaction was completed, a saturated NH_4Cl aqueous solution was added. The organic layer was separated and the aqueous layer was extracted with CH_2Cl_2 three times. The combined organic layer was dried over Na_2SO_4, filtered, and concentrated under reduced pressure. The product was purified by column chromatography (PE). Yield: 94 %. The crystal sample was recrystallization from tetrahydrofuran.

^{1}H NMR (400 MHz, $CDCl_3$): δ 7.89 (d, 2H), 7.16 (d, 2H), 7.00 (t, 2H), 6.86 (d, 2H), 6.74 (s, 4H) , 2.25 (s, 6H), 1.94 (s, 12H); ^{13}C NMR (100 MHz, $CDCl_3$): δ 143.28, 141.04, 139.17, 138.19, 128.72, 128.09,126.24, 122.59, 119.44, 115.46, 21.92, 21.30. HRMS, m/z: [M$^+$] calcd for $C_{30}H_{30}BN$, 415.2471; found, 415.2475; elemental analysis calcd (%) for $C_{30}H_{30}BN$: C, 86.75; H, 7.28; N, 3.37; found: C, 86.57; H, 7.11; N, 3.20. Mp (°C) of **BCz** crystal: 255.1 ~ 256.2.

Synthesis of 9-trityl-9*H*-carbazole (CCz).

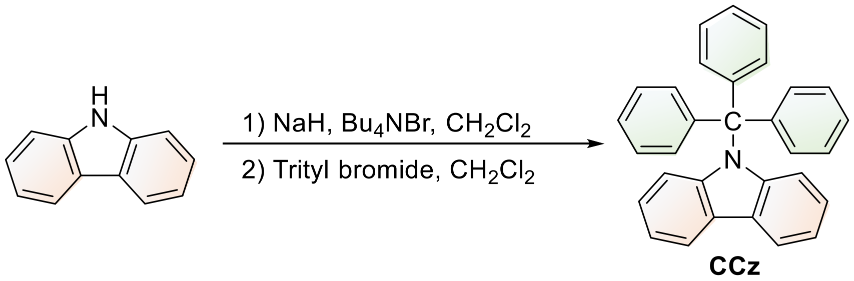

To a solution of carbazole (0.836 g, 5.0 mmol) in CH_2Cl_2 (25 mL) was added Bu_4NBr (0.05 g, 0.15 mmol) and NaH (0.36 g, 15 mmol). After the reaction mixture was stirred at room temperature for 30 min, trityl bromide (0.970g, 3.0 mmol) in 5 mL CH_2Cl_2 was added to the mixture in three times with each 30 min The reaction mixture was stirred for 2 h. After the reaction was completed, the mixture was extracted with ethyl acetate. The organic layer was dried over Na_2SO_4, filtered, and concentrated under reduced pressure. The product was purified by column chromatography (PE/DCM) and recrystallized with THF. Yield: 61 %.

^{1}H NMR (400 MHz, $CDCl_3$): δ 8.06 (d, 2H), 7.40 (d, 2H), 7.36-7.32 (m, 4H), 7.27 (t, 6H), 7.21-7.13 (m, 9H); ^{13}C NMR (100 MHz, $CDCl_3$): δ 143.56, 143.17, 140.84, 135.81, 130.78, 129.46, 128.49, 126.80, 126.56, 125.84, 123.31, 120.25, 119.84, 109.83. HRMS, m/z: [M$^+$] calcd for $C_{31}H_{23}N$, 409.1830; found, 409.1825; elemental analysis calcd (%) for $C_{31}H_{23}N$: C, 90.92; H, 5.66; N, 3.42; found: C, 90.69; H, 5.85; N, 3.52. Mp (°C) of **CCz** crystal: 190.3 ~ 191.5.

Synthesis of N,N-diphenyl-9*H*-carbazol-9-amine (NCz).

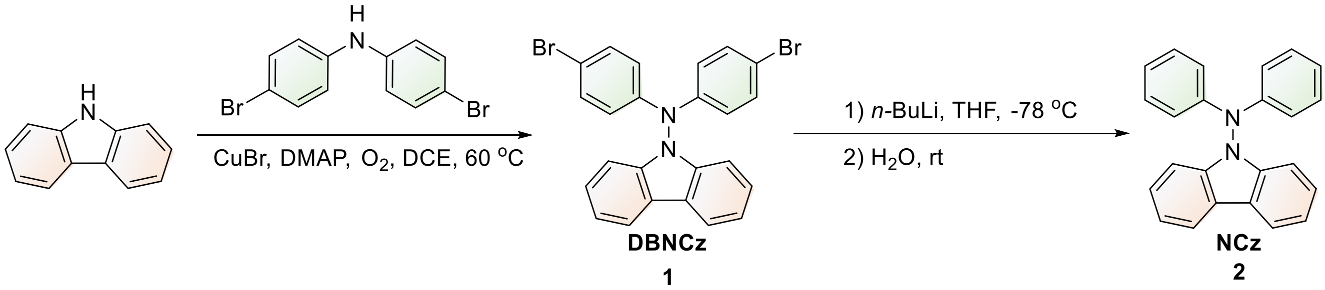

(1) To a 50ml vial with stir bar was charged with carbazole (0.502 g, 3.0 mmol), 4,4′-Dibromodiphenylamine (0.654 g, 2.0 mmol), CuBr (0.029 g, 0.2 mmol) and DMAP (0.049 g, 0.4 mmol). After the vial was purged with O_2 for 10 min, 10 mL 1,2-dichloroethane was added *via* syringe, and the reaction mixture was stirred at 60 °C for 17 h. After 17 h, the reaction was cooled to room temperature, diluted with DCM and washed with saturated aqueous NH_4Cl. The organic layer was washed with water, dried over Na_2SO_4, filtered, and concentrated under reduced pressure. The product was purified by column chromatography (PE/DCM). Yield: 40 %.

^{1}H NMR (400 MHz, $CDCl_3$): δ 8.04 (d, 2H), 7.31 (t, 2H), 7.24-7.20 (m, 8H), 6.87-6.84 (m, 4H); ^{13}C NMR (100 MHz, $CDCl_3$): δ 143.12, 138.90, 132.43, 126.56, 121.50, 120.93, 120.67, 120.09, 115.74, 109.00.

(2) To a solution of **DBNCz** (0.591 g, 1.2 mmol) in THF (25 mL) was added *n*-BuLi (2.50 M in hexane, 1.20 mL, 3 mmol) dropwise at -78 °C. The reaction mixture was gradually warmed to room temperature and then stirred overnight. After the reaction was completed, H_2O was added. The organic layer was washed with saturated aqueous NaCl and dried over Na_2SO_4, filtered, and concentrated under reduced pressure. The product was purified by column chromatography (PE/DCM). Yield: 90 %. The crystal sample was recrystallization from tetrahydrofuran.

^{1}H NMR (400 MHz, $CDCl_3$): δ 8.04 (d, 2H), 7.30 (d, 4H), 7.22-7.18 (m, 2H), 7.15-7.11 (m, 4H),7.01 (d, 4H), 6.90 (t, 2H); ^{13}C NMR (100 MHz, $CDCl_3$): δ 144.42, 139.40, 129.31, 126.43, 122.94, 121.40, 120.50, 120.47, 118.49, 109.34. HRMS, m/z: [M^+] calcd for $C_{24}H_{18}N_2$, 334.1470; found, 334.1460; elemental analysis calcd (%) for $C_{24}H_{18}N_2$: C, 86.20; H, 5.43; N, 8.38; found: C, 86.06; H, 5.45; N, 8.19. Mp (°C) of **NCz** crystal: 168.9 ~ 169.9.

Synthesis of 9-(phenylthio)-9*H*-carbazole (SOCz).

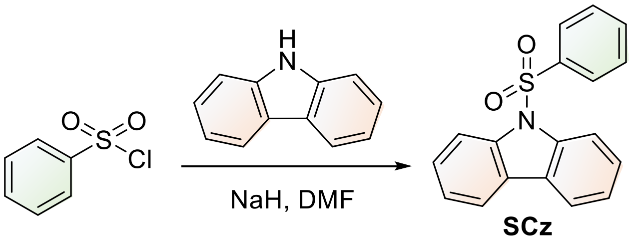

A solution of carbazole (1.67 g, 10.0 mmol) in dry DMF (20 mL) was added to a solution of sodium hydride (0.288 g, 12.0 mmol) in dry DMF (15 mL) at room temperature. After the reaction mixture was stirred at room temperature for 30 min, benzenesulphonylchloride (1.767 g, 10.0 mmol) in 5 mL dry DMF was added, the mixture was stirred at room temperature for 5 h. The organic layer was washed with saturated aqueous NaCl, saturated aqueous $NaHCO_3$, and dried over Na_2SO_4, filtered, and concentrated under reduced pressure. The product was purified by column chromatography (PE/DCM). Yield: 90 %. The crystal sample was recrystallization from tetrahydrofuran.

^{1}H NMR (400 MHz, $CDCl_3$): δ 8.25 (d, 2H), 7.81 (d, 2H), 7.73 (d, 2H), 7.41 (t, 2H), 7.34 (t, 1H), 7.28 (t, 2H), 7.21 (t, 2H); ^{13}C NMR (100 MHz, $CDCl_3$): δ 138.30, 137.82, 133.75, 129.00, 127.40, 126.40, 126.37, 123.96, 120.00, 115.09. HRMS, m/z:

[M$^+$] calcd for $C_{18}H_{13}NO_2S$, 307.0667; found, 307.0660; elemental analysis calcd (%) for $C_{18}H_{13}NO_2S$: C, 70.34; H, 4.26; N, 4.56; S, 10.43; found: C, 70.14; H, 4.32; N, 4.53; S, 10.51. Mp (°C) of **SOCz** crystal: 126.1 ~ 127.4.

Synthesis of 9-(phenylthio)-9*H*-carbazole (SCz).

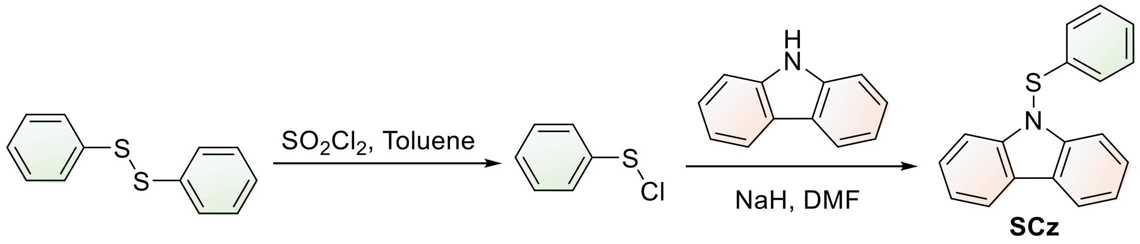

To a solution of diphenyl disulfide (2.18 g, 10 mmol) in toluene (15 mL) was added sulfuryl chloride (1.23 g, 9.1 mmol) dropwise at 0 °C. The reaction mixture was gradually warmed to room temperature and then stirred 20 min. Then, to a solution of carbazole (2.01 g, 10 mmol) in toluene (15 mL) was added the sodium hydride (0.576 g, 24.0 mmol) in toluene (10 mL) at room temperature and stirred for 30 min. This was followed by the dropwise addition of the solution of diphenyl disulfide and sulfuryl chloride mixture at 0 °C. After the reaction was completed, ethyl acetate was added. The organic layer was washed with saturated aqueous NaCl and dried over Na_2SO_4, filtered, and concentrated under reduced pressure. The product was purified by column chromatography (PE/DCM). Yield: 81 %. The crystal sample was recrystallization from tetrahydrofuran. ^{1}H NMR (400 MHz, $CDCl_3$): δ 7.99 (d, 2H), 7.66 (d, 2H), 7.40 (t, 2H), 7.24 (t, 2H), 7.11 (t, 2H), 7.05 (m, 1H), 6.91 (d, 2H); ^{13}C NMR (100 MHz, $CDCl_3$): δ 143.34, 137.95, 129.17, 126.67, 126.54, 124.59, 124.04, 121.35, 120.25, 111.07. HRMS, m/z: [M$^+$] calcd for $C_{18}H_{13}NS$, 275.0769; found, 275.0758; elemental analysis calcd (%) for $C_{18}H_{13}NS$: C, 78.51; H, 4.76; N, 5.09; S, 11.64; found: C, 78.34; H, 4.78; N, 4.98; S, 11.36. Mp (°C) of **SCz** crystal: 91.8 ~ 93.2.

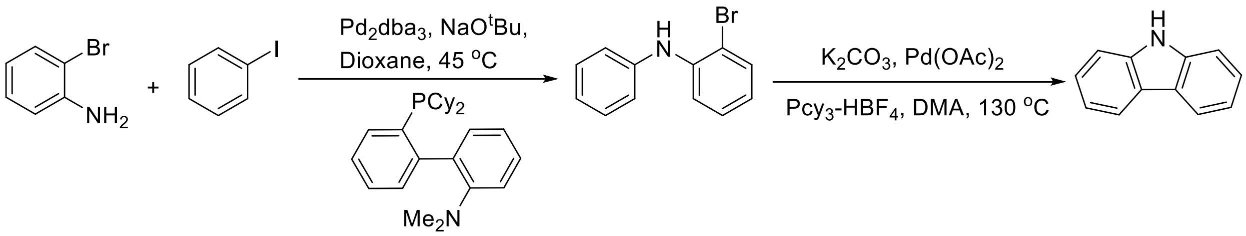

Scheme S1 The synthetic route of carbazole.

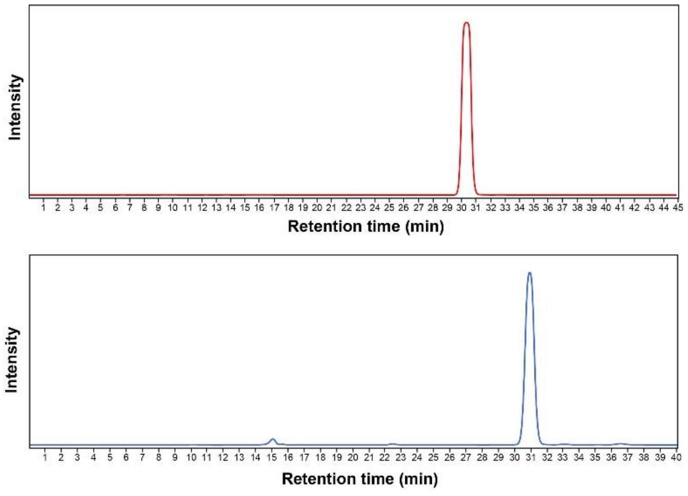

Fig. S1 The HPLC profiles of lab synthesized carbazole (red line) and commercial carbazole (blue line).

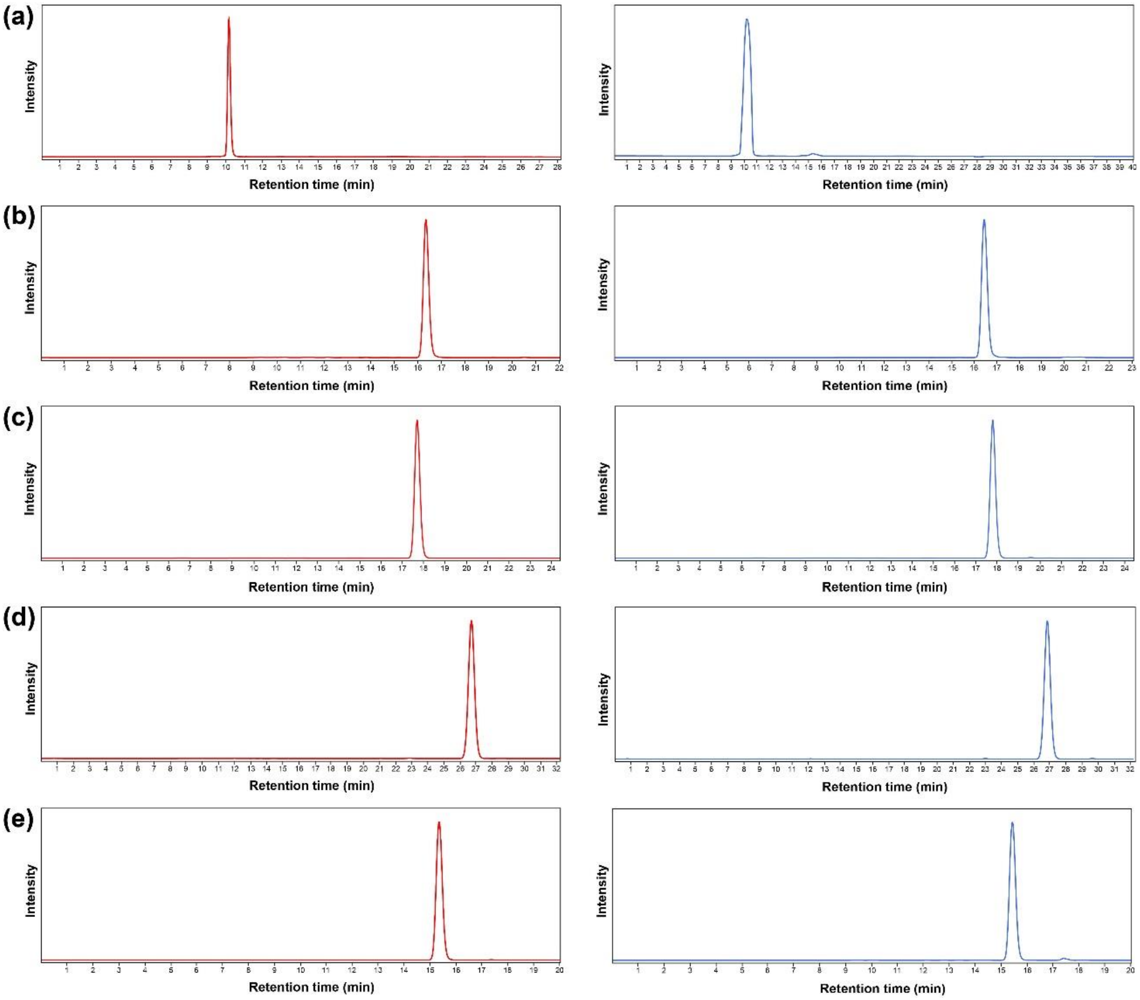

Fig. S2 The HPLC profiles of **XCz**-Lab (red lines) and **XCz**-Cm (blue lines), (a) **BCz**, (b) **CCz**, (c) **NCz**, (d) **SOCz** and (6) **SCz**, respectivly.

3. UV-vis, excitation and emission spectra of XCz-Cm in solution

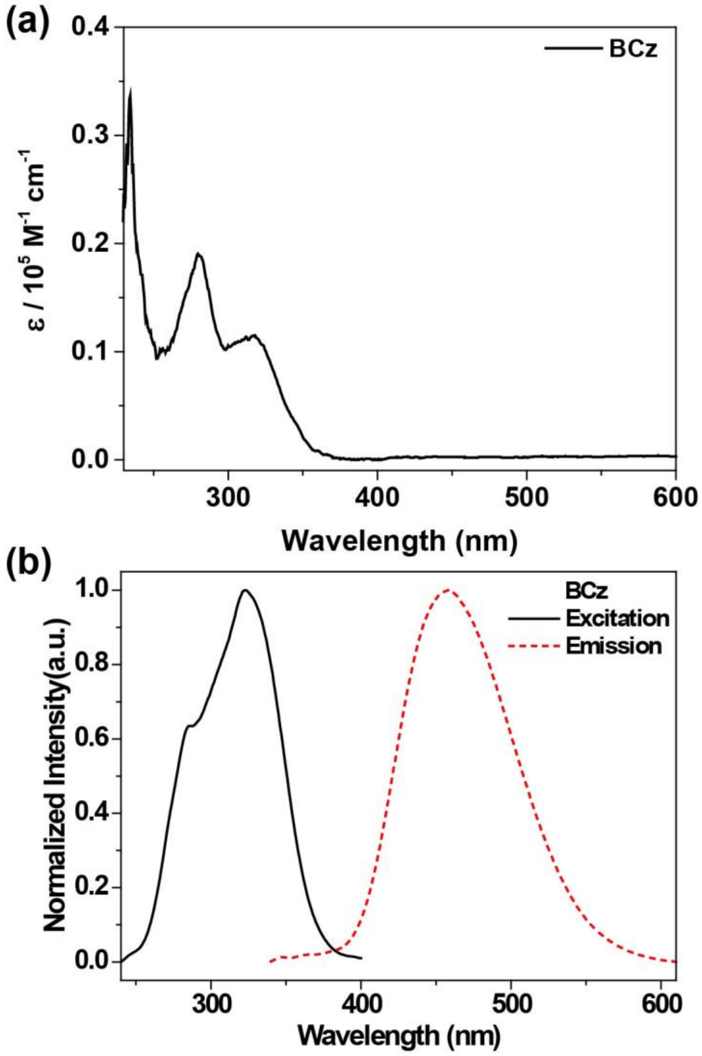

Fig. S3 Photophysical spectra for **BCz**-Cm in THF. (a) UV-Vis absorbance spectrum; (b) fluorescence excitation (solid line) and emission spectra (dashed line). [**BCz**] = 2 × 10^{-5} M.

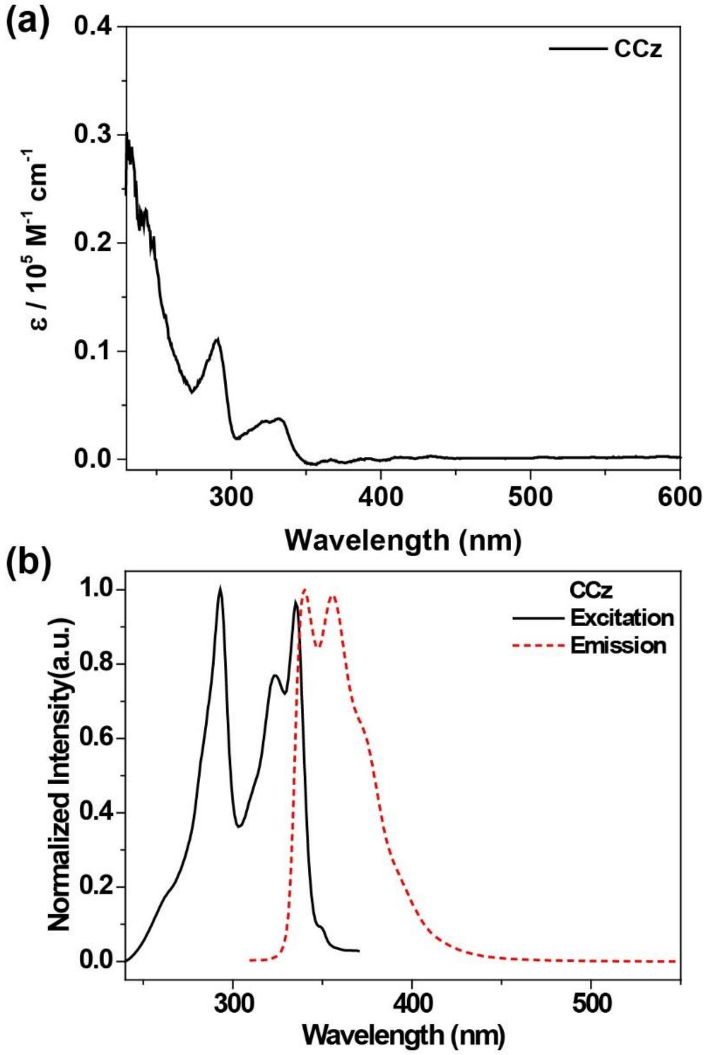

Fig. S4 Photophysical spectra for **CCz**-Cm in THF. (a) UV-Vis absorbance spectrum; (b) fluorescence excitation (solid line) and emission spectra (dashed line). [**CCz**] = 2 × 10^{-5} M.

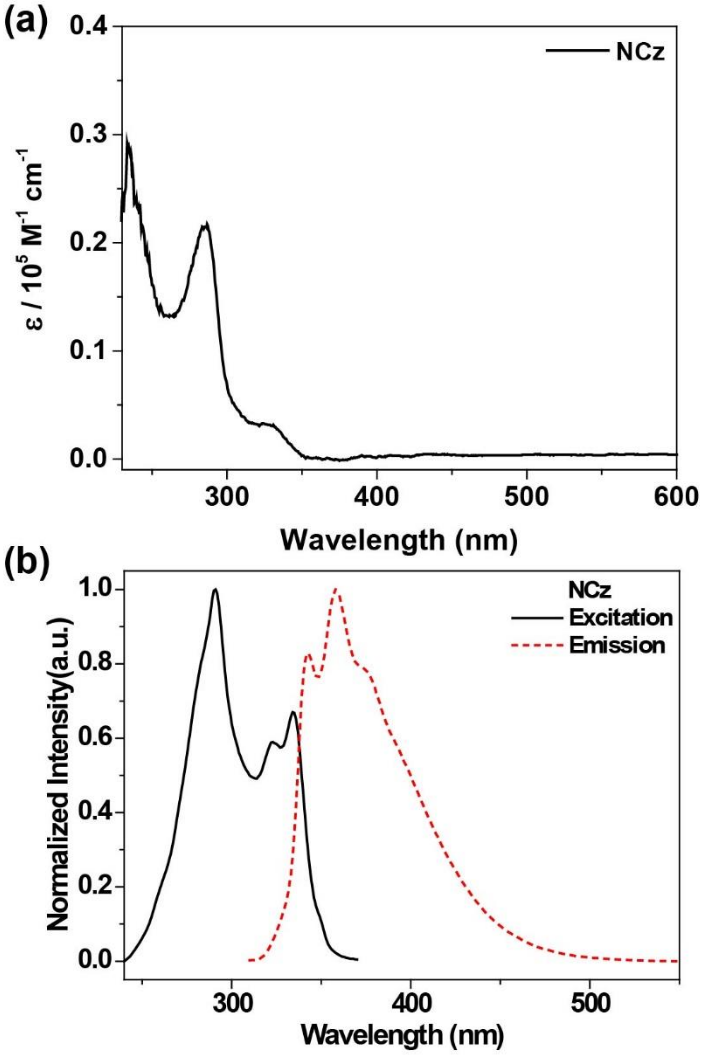

Fig. S5 Photophysical spectra for **NCz**-Cm in THF. (a) UV-Vis absorbance spectrum; (b) fluorescence excitation (solid line) and emission spectra (dashed line). [**NCz**] = 2 × 10^{-5} M.

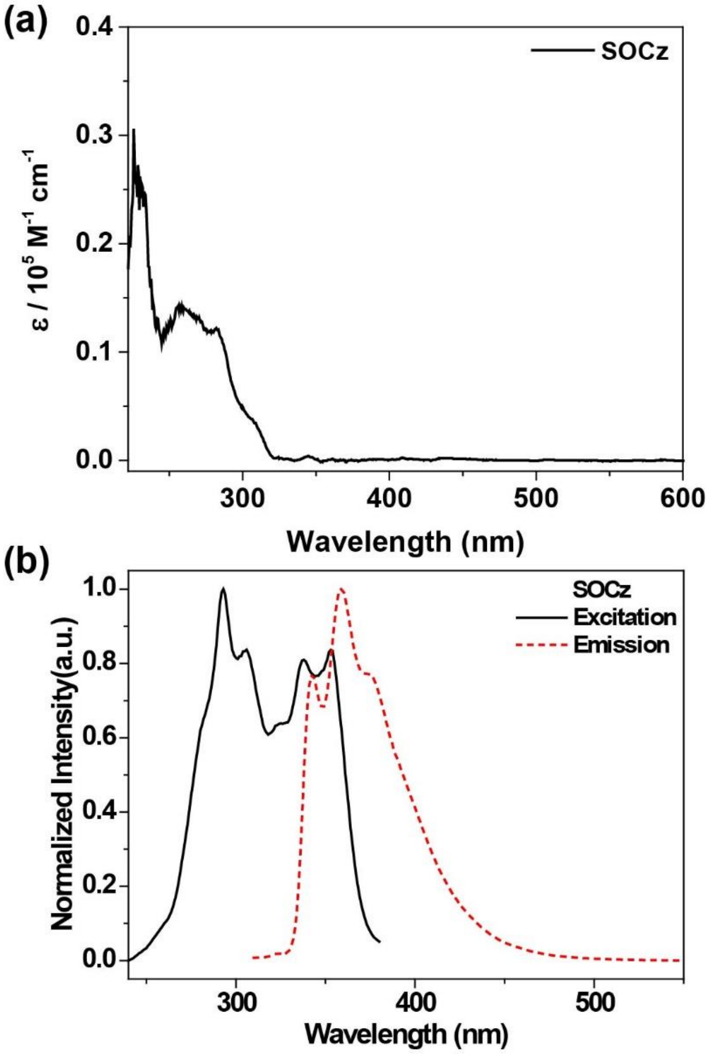

Fig. S6 Photophysical spectra for **SOCz**-Cm in THF. (a) UV-Vis absorbance spectrum; (b) fluorescence excitation (solid line) and emission spectra (dashed line). [**SOCz**] = 2 × 10^{-5} M.

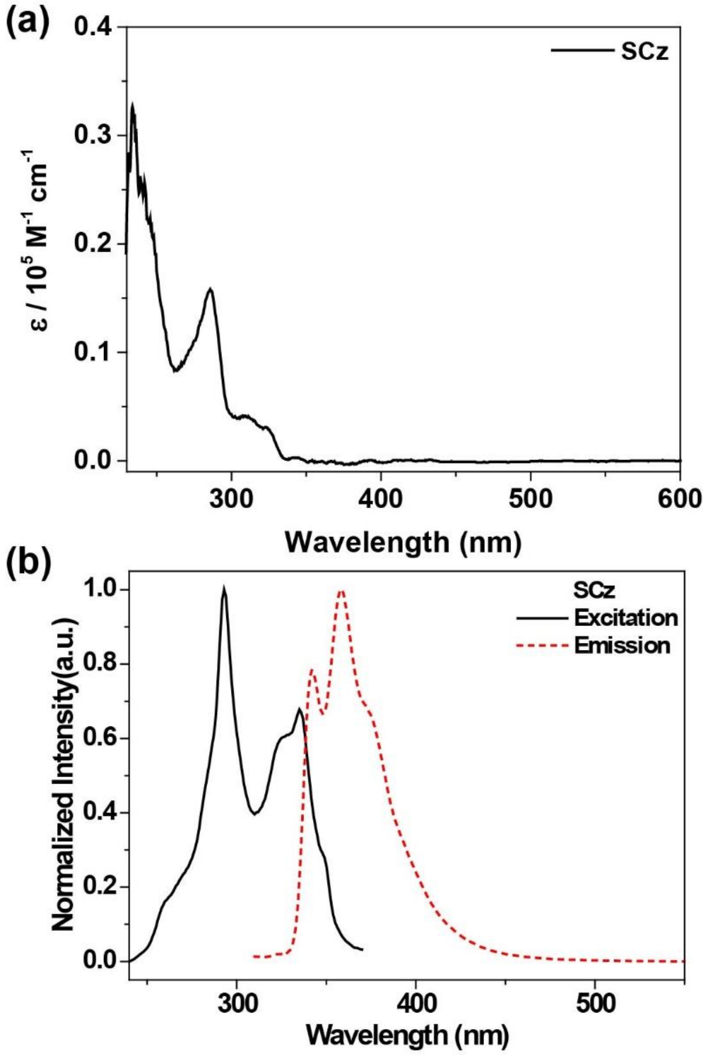

Fig. S7 Photophysical spectra for **SCz**-Cm in THF. (a) UV-Vis absorbance spectrum; (b) fluorescence excitation (solid line) and emission spectra (dashed line). [**SCz**] = 2 × 10^{-5} M.

Table S1 Summarized absorption and emission data of **XCz**-Cm in solution.

Compound	Absorption		Emission wavelength					
	λ_{ab} (nm)	ε [$10^5(M^{-1}cm^{-1})$]	Cyclohexane	Toluene	DCM	THF	Chloroform	MeCN
BCz	234	0.336	432	446	457	458	459	409
	297	0.191	-	-	-	-	-	432
	317	0.115	-	-	-	-	-	506
CCz	227	0.338	338	340	341	340	342	340
	291	0.110	353	335	357	356	357	356
	331	0.038	-	-	-	-	-	-
NCz	233	0.292	333	340	338	343	410	397
	286	0.217	351	356	354	358	436	-
	324	0.033	363	371	372	-	459	-
	-	-	-	-	390	-	-	-
SOCz	225	0.306	334	340	338	343	340	408
	256	0.139	351	356	354	358	383	415
	282	0.122	366	371	369	374		430
SCz	233	0.327	333	339	338	342	357	405
	286	0.158	350	355	354	358	371	517
	323	0.031	365	-	369	-	-	-

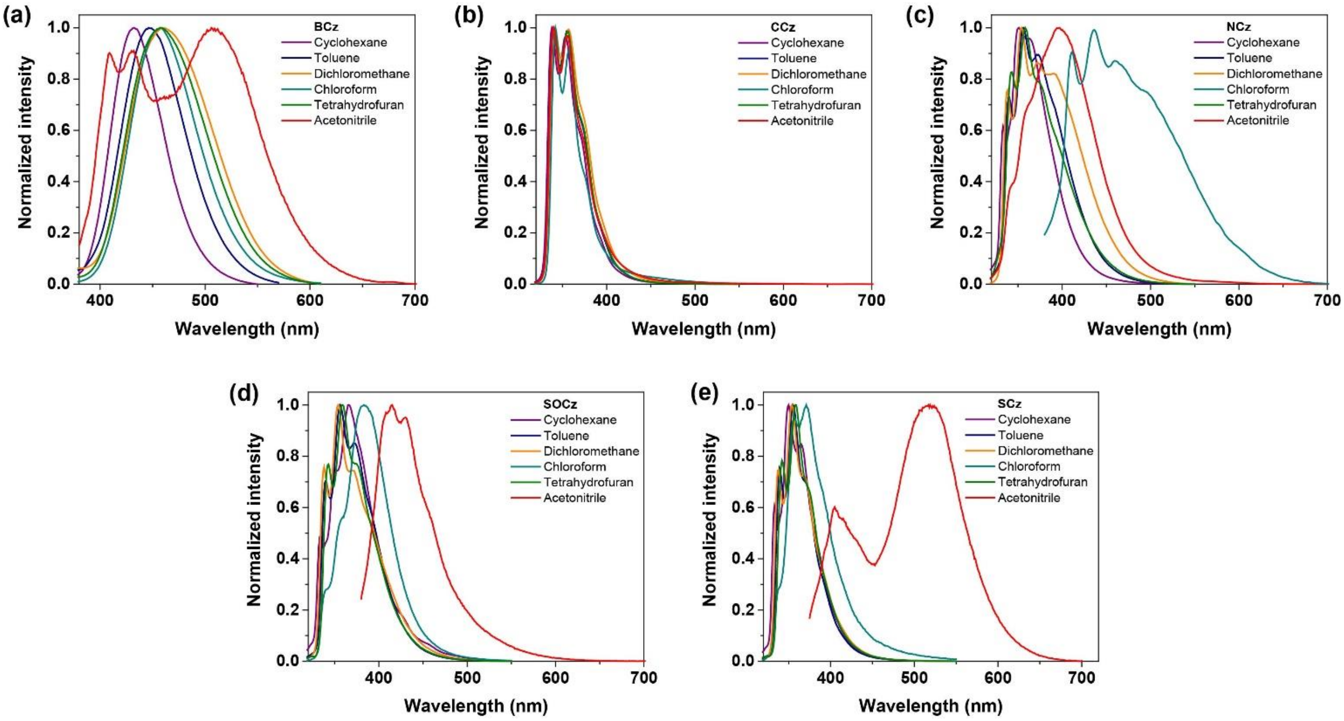

Fig. S8 Photophysical properties of (a) **BCz**-Cm, (b) **CCz**-Cm, (c) **NCz**-Cm, (d) **SOCz**-Cm and (e) **SCz**-Cm in different solutions. PL spectra of **BCz**-Cm, **CCz**-Cm, **NCz**-Cm, **SOCz**-Cm, and **SCz**-Cm in six types of solvents (cyclohexane, toluene, dichloromethane, tetrahydrofuran, chloroform and acetonitrile) at room temperature.

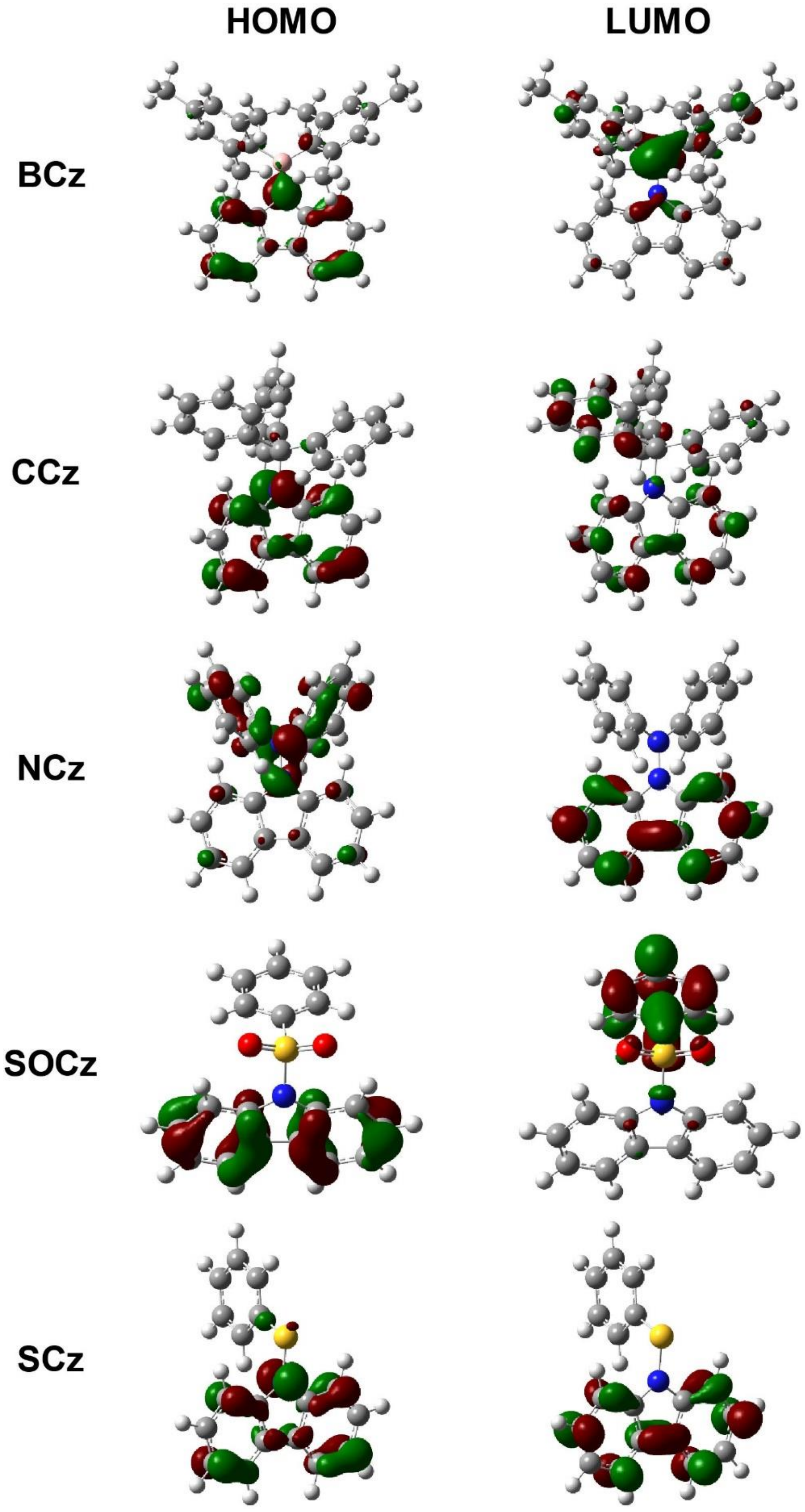

Fig. S9 Electrical density contour of HOMO and LUMO of **XCz** in the gas phase (contour level=0.05).

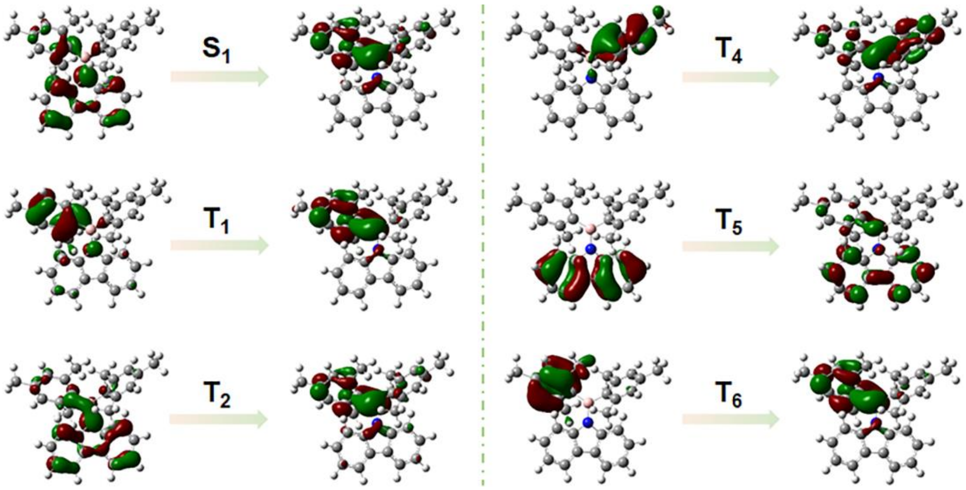

Fig. S10 The NTOs for excited states at single crystal geometric structures of **BCz** are obtained by the density functional method at the B3LYP/6-31G(d) level.

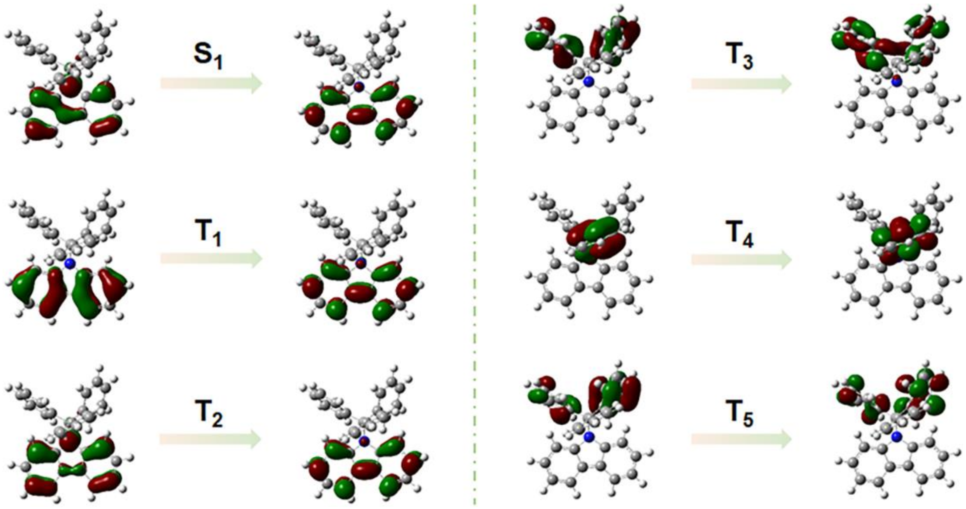

Fig. S11 The NTOs for excited states at single crystal geometric structures of **CCz** are obtained by the density functional method at the B3LYP/6-31G(d) level.

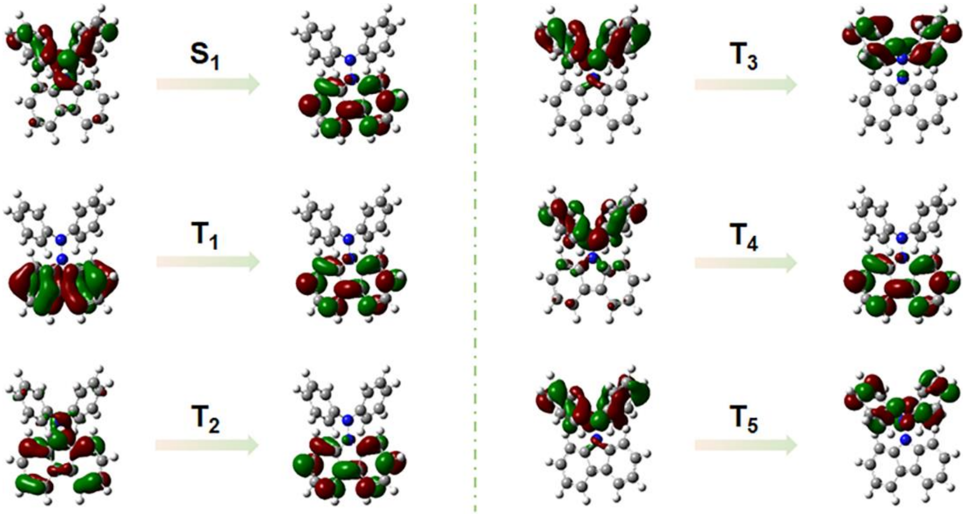

Fig. S12 The NTOs for excited states at single crystal geometric structures of **NCz** are obtained by the density functional method at the B3LYP/6-31G(d) level.

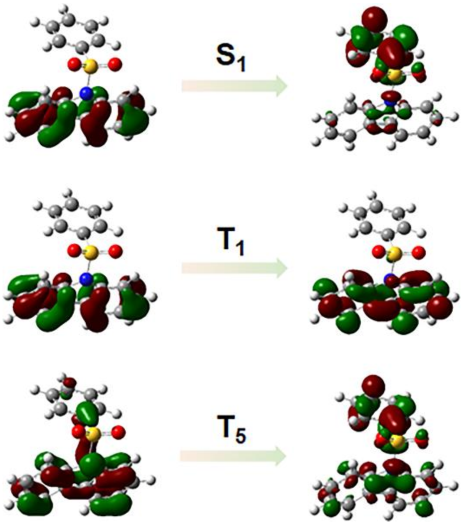

Fig. S13 The NTOs for excited states at single crystal geometric structures of **SOCz** are obtained by the density functional method at the B3LYP/6-31G(d) level.

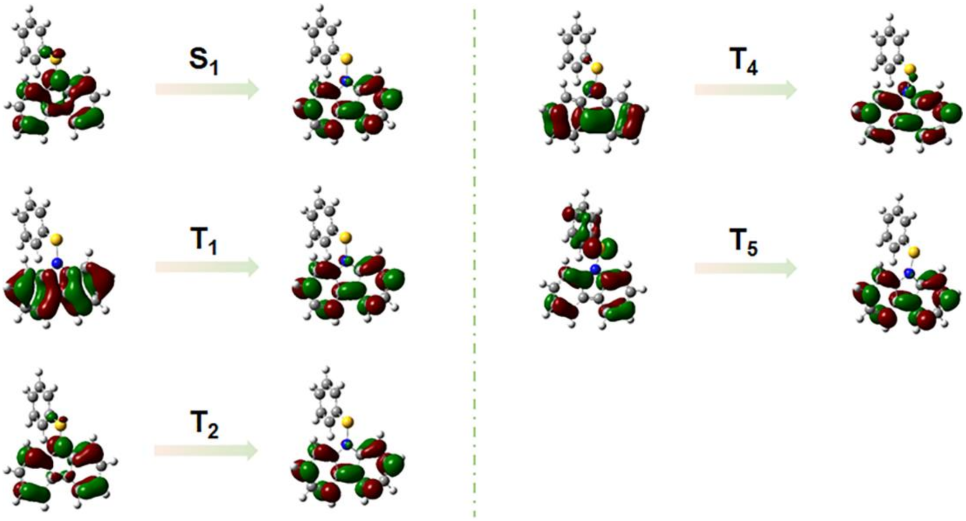

Fig. S14 The NTOs for excited states at single crystal geometric structures of **SCz** are obtained by the density functional method at the B3LYP/6-31G(d) level.

4. Phosphorescence spectra of XCz-Cm in 2-Me-THF at 77 K

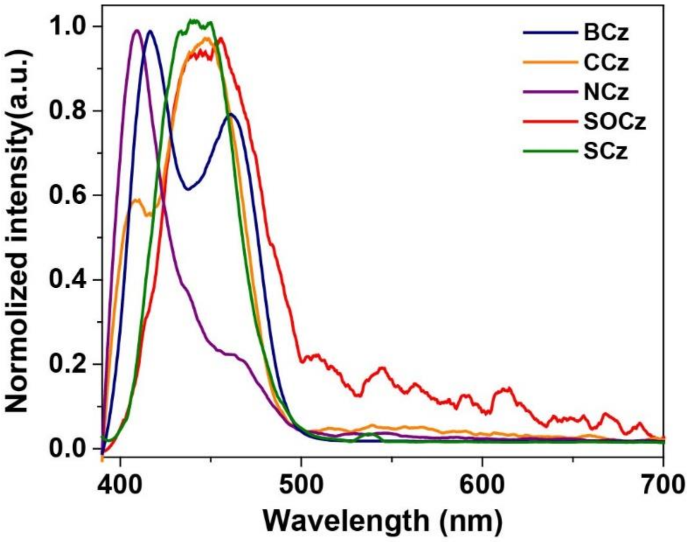

Fig. S15 Phosphorescence spectra of **BCz**-Cm, **CCz**-Cm, **NCz**-Cm, **SOCz**-Cm and **SCz**-Cm in 2-Me-THF (1.0 × 10^{-3} M) at 77 K. Excitation wavelength: 365 nm.

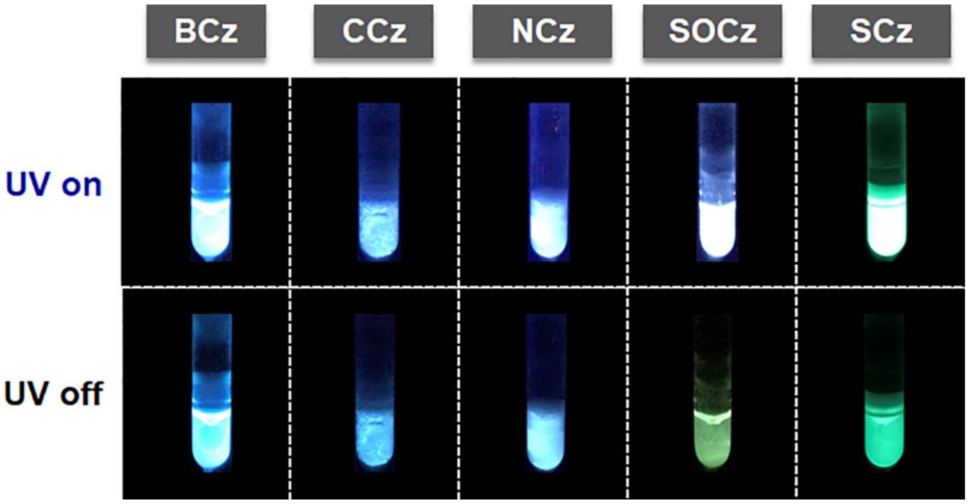

Fig. S16 Photographs of **BCz**-Cm, **CCz**-Cm, **NCz**-Cm**, SOCz**-Cm and **SCz**-Cm in dilute 2-Me-THF solution (1.0 × 10^{-3} M) at 77 K before and after excitation light source at 365 nm was switched off.

5. PL and phosphorescence spectra, photographs of Cz-Cm, Cz-Lab, XCz-Cm and XCz-Lab

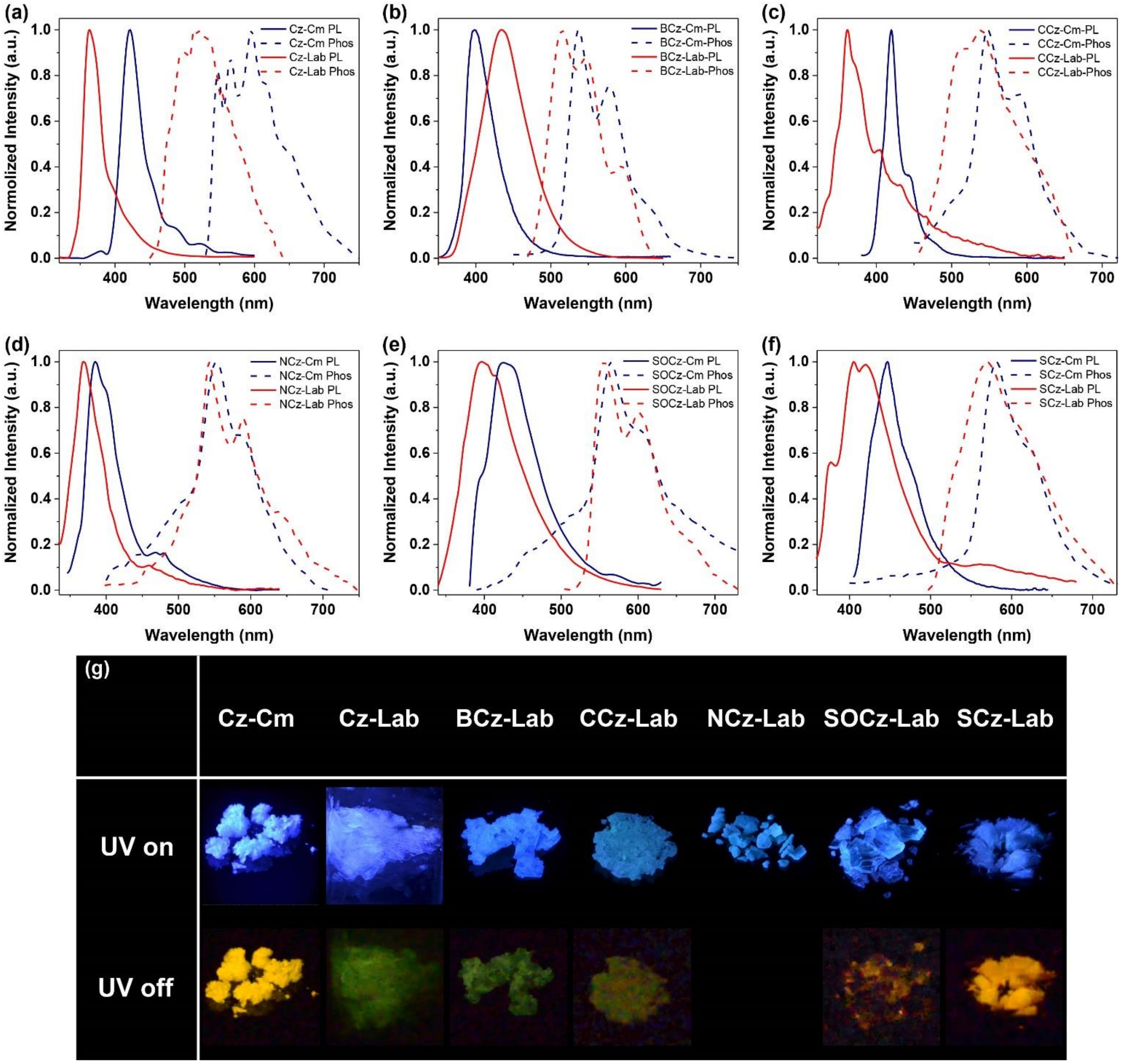

Fig. S17 The photoluminescence (blue lines) and phosphorescence (red lines) spectra of (a) Cz-Cm and Cz-Lab, (b-f) **XCz**-Cm and **XCz**-Lab. (g) Photographs of Cz-Cm, Cz-Lab, **XCz**-Cm and **XCz**-Lab before and after 365 nm irradiation.

6. CIE chromaticity diagram signifying the phosphorescent color of XCz-Cm crystals

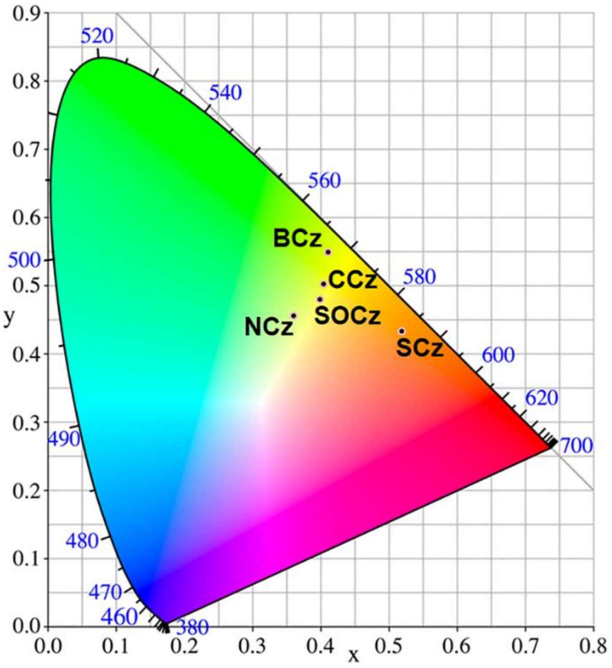

Fig. S18 CIE chromaticity diagram signifying the phosphorescent color coordinates for the **XCz**-Cm crystals (**BCz**-Cm (0.41, 0.55), **CCz**-Cm (0.40, 0.50), **NCz**-Cm (0.36, 0.45), **SOCz**-Cm (0.40, 0.48), **SCz**-Cm (0.51, 0.43)).

7. UOP spectra of XCz-Cm in the air and argon

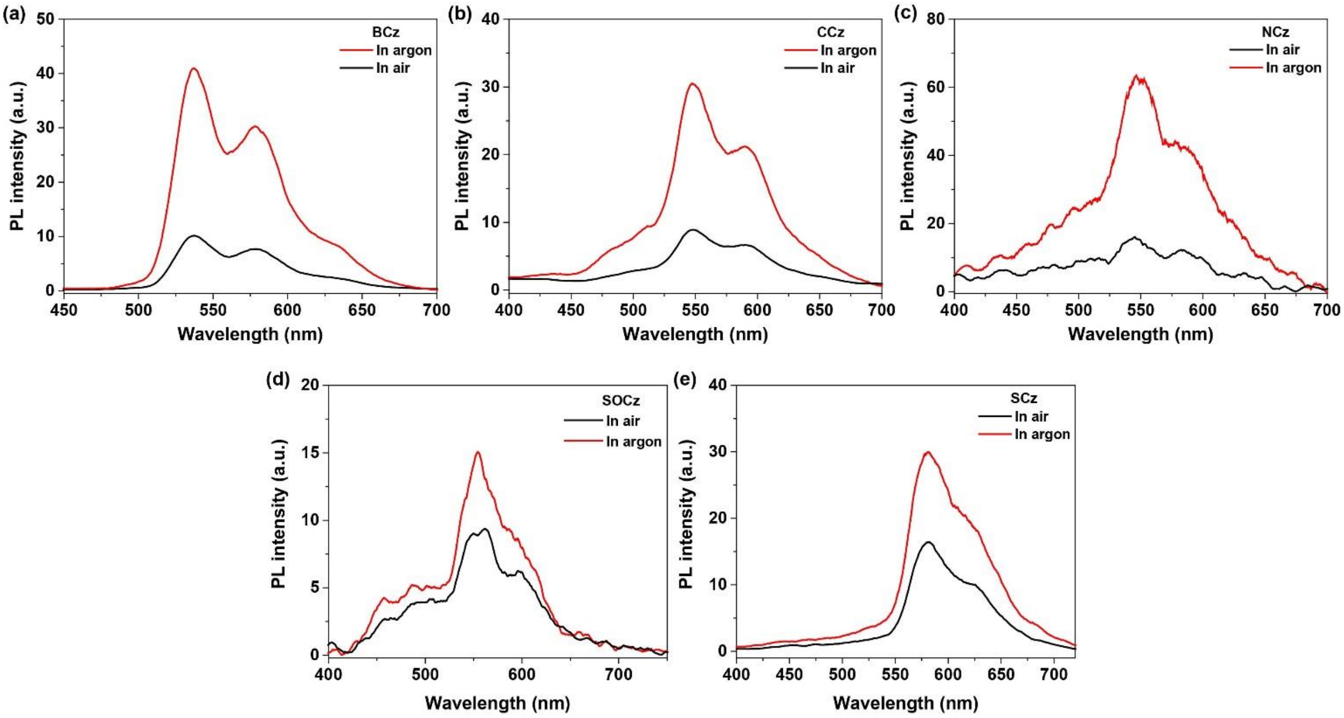

Fig. S19 Phosphorescence spectra at room temperature of **XCz**-Cm in air and argon atmosphere respectively. Excitation wavelength: 365 nm.

8. Lifetime decay profiles and luminescence data of XCz-Cm and XCz-Lab in crystalline state

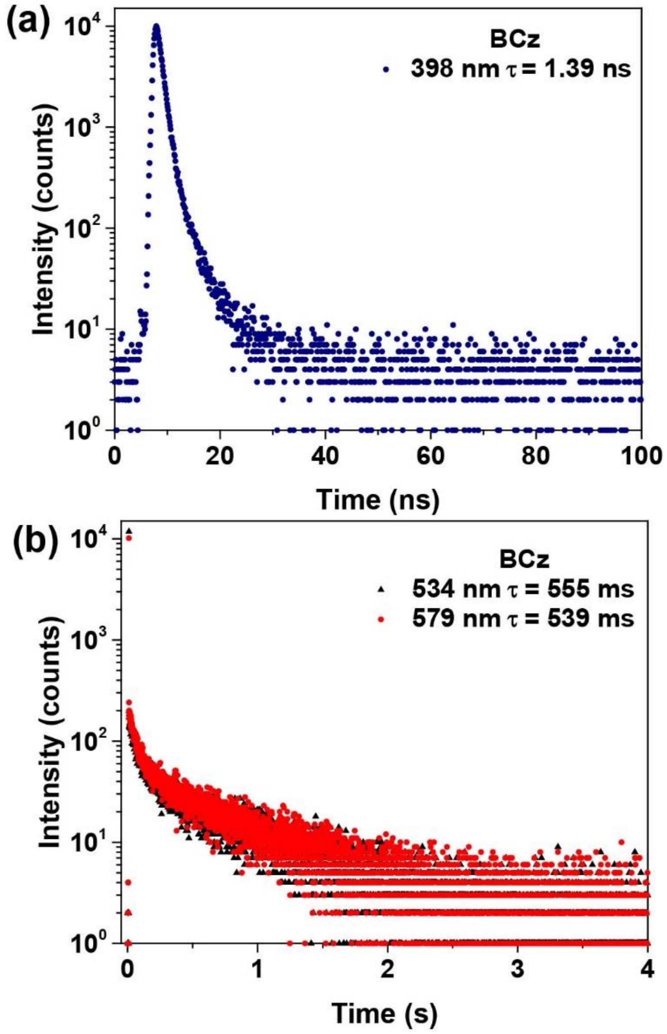

Fig. S20 Lifetime decay profiles of (a) the fluorescence emission bands and (b) the ultralong phosphorescence bands of **BCz**-Cm crystalline powders under ambient conditions.

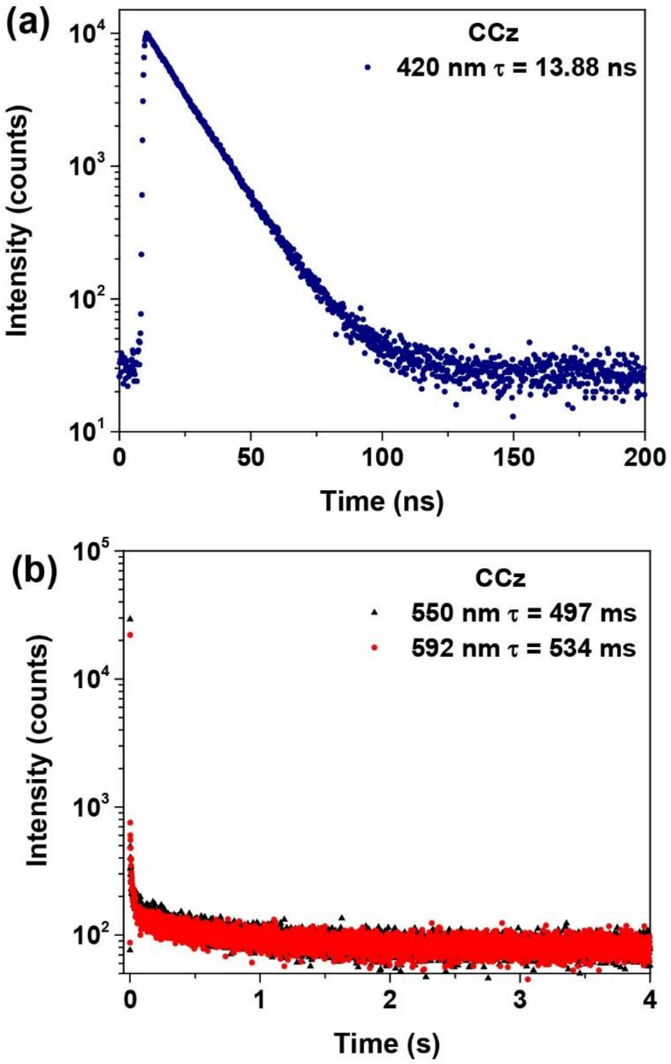

Fig. S21 Lifetime decay profiles of (a) the fluorescence emission bands and (b) the ultralong phosphorescence bands of **CCz**-Cm crystalline powders under ambient conditions.

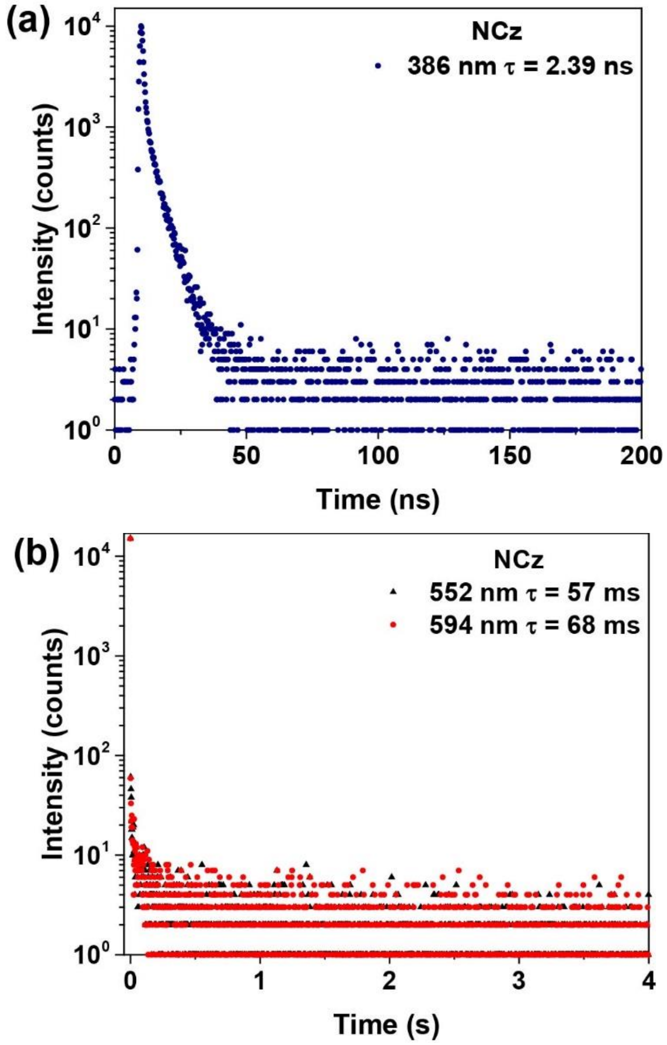

Fig. S22 Lifetime decay profiles of (a) the fluorescence emission bands and (b) the ultralong phosphorescence bands of **NCz**-Cm crystalline powders under ambient conditions.

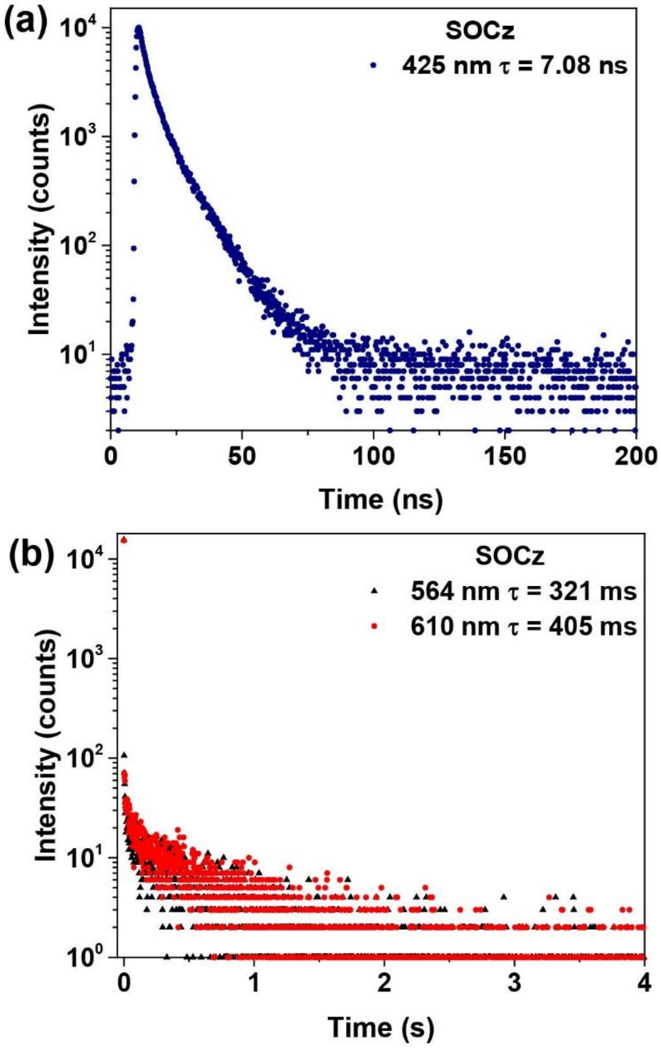

Fig. S23 Lifetime decay profiles of (a) the fluorescence emission bands and (b) the ultralong phosphorescence bands of **SOCz**-Cm crystalline powders under ambient conditions.

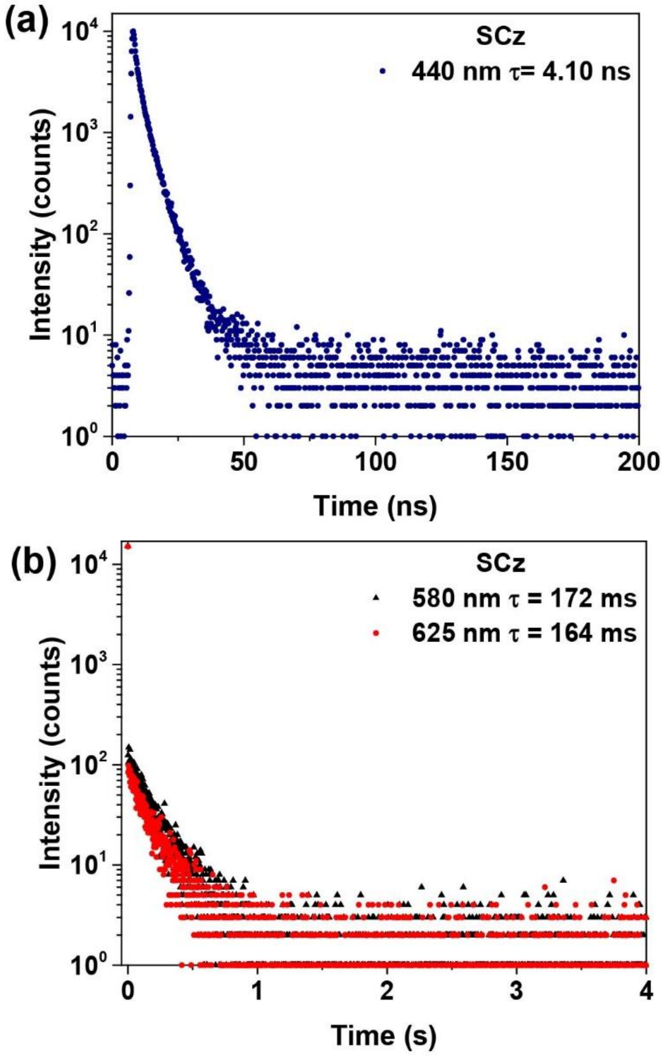

Fig. S24 Lifetime decay profiles of (a) fluorescence emission bands and (b) the ultralong phosphorescence bands of **SCz**-Cm crystalline powders under ambient conditions.

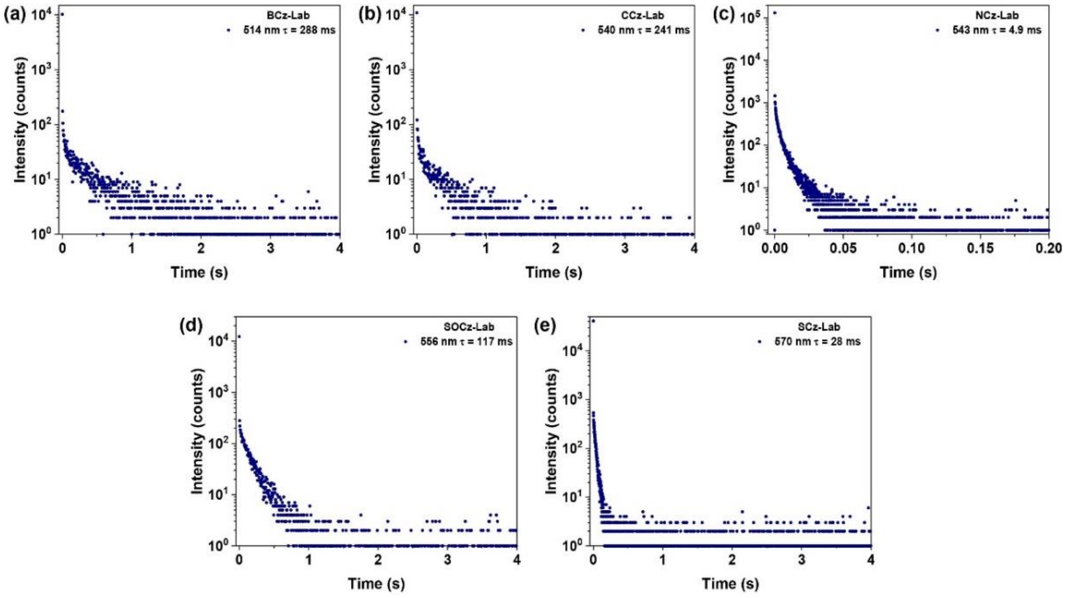

Fig. S25 Lifetime decay profiles of ultralong phosphorescence bands of (a-e) **BCz**-Lab, **CCz**-Lab, **NCz**-Lab, **SOCz**-Lab, **SCz**-Lab crystalline powders under ambient conditions, respectively.

Table S2 Photoluminescence lifetimes (τ) of **XCz**-Cm in the crystalline state.

Compound	Wavelength (nm)	Fluorescence				Phosphorescence			
		τ_1 (ns)	A_1 (%)	τ_2 (ns)	A_2 (%)	τ_1 (ms)	A_1 (%)	τ_2 (ms)	A_2 (%)
BCz	398	1.00	87.34	4.04	12.66	-	-	-	-
	534	-	-	-	-	60.54	19.36	673.40	80.64
	579	-	-	-	-	58.35	19.69	657.06	80.31
CCz	420	13.88	100%	-	-	-	-	-	-
	550					16.22	5.71	526.21	94.29
	592					11.53	10.77	596.50	89.23
NCz	386	0.68	55.36	4.52	44.64				
	552					57.13	100		
	594					67.77	100		
SOCz	425	2.96	44.99	10.44	55.01				
	564					12.48	11.33	360.99	88.67
	610					28.43	12.22	460.44	87.78
SCz	440	2.18	48.21	5.87	51.79				
	580					110.39	47.95	228.80	52.05
	625					101.42	49.93	225.41	50.07

Table S3 Phosphorescence lifetimes (τ) of **XCz**-Lab in the crystalline state.

Compound	Wavelength (nm)	Phosphorescence			
		τ_1 (ms)	A_1 (%)	τ_2 (ms)	A_2 (%)
BCz	514	22.81	14.45	334.31	85.55
CCz	540	16.98	14.48	279.02	85.52
NCz	543	1.34	44.61	7.68	55.39
SOCz	564	20.48	12.05	130.92	87.95
SCz	570	7.60	14.71	31.50	85.29

Determined from the fitting function of $I(t) = A_1 e^{-\frac{t}{\tau_1}} + A_2 e^{-\frac{t}{\tau_2}}$ according to the fluorescence and ultralong luminescence decay curves.

The photoluminescence quantum yield of **XCz**-Cm were 6.80% (**BCz**-Cm), 16.50% (**CCz**-Cm), 3.25% (**NCz**-Cm), 1.76% (**SOCz**-Cm), 1.22% (**SCz**-Cm).

The photoluminescence quantum yield of **XCz**-Lab were 4.01% (**BCz**-Lab), 11.84% (**CCz**-Lab), 2.91% (**NCz**-Lab), 0.44% (**SOCz**-Lab), 0.28% (**SCz**-Lab).

9. Single-crystal X-ray structure determination

X-ray Crystallography. Crystals of appropriate quality for X-ray diffraction studies were selected a suitable crystal, attached to a glass fiber, and quickly placed in a glass vial. All data were collected using a Bruker APEX II CCD detector/D8 diffractometer using Mo/Cu Kα radiation. The data were corrected for absorption through Gaussian integration from indexing of the crystal faces. Structures were solved using the direct methods programs SHELXS-97, and refinements were completed using the program SHELXL-97.

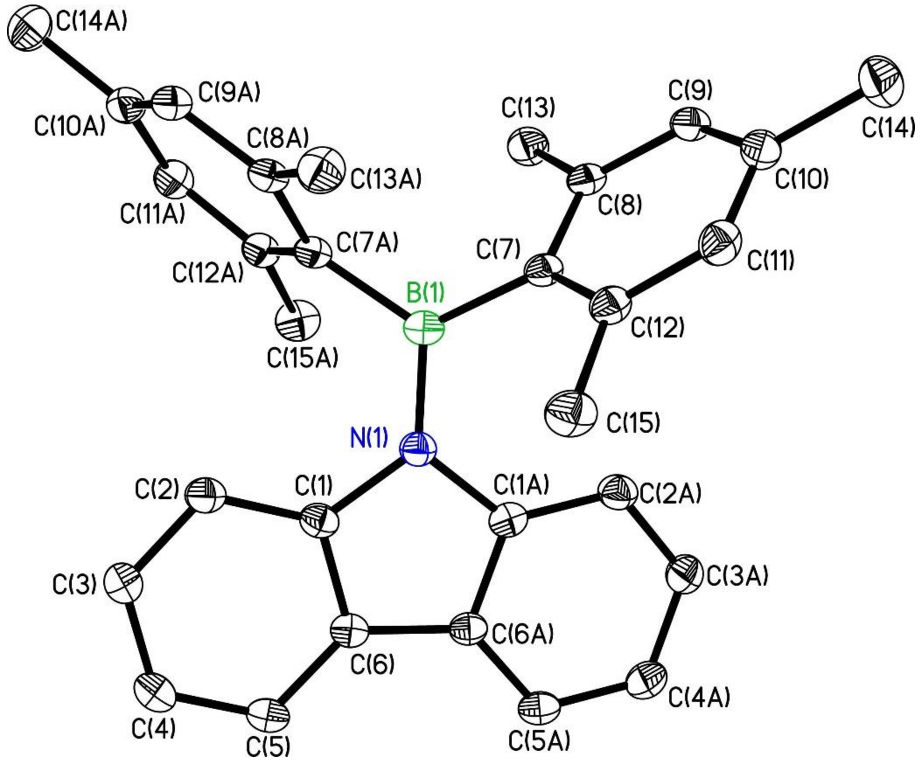

Fig. S26 Molecular Structure of **BCz** with thermal ellipsoids presented at a 50% probability level. All hydrogen atoms have been omitted for clarity. Selected bond lengths (Å): N(1)-C(1A), 1.420(2); N(1)-C(1), 1.420(2); N(1)-B(1), 1.435(4); C(7)-B(1), 1.567(2); B(1)-C(7A), 1.567(2); C(8)-C(13), 1.502(3); C(12)-C(15), 1.504(3); C(10)-C(14), 1.495(3). Bond angles (deg): C(1A)-N(1)-C(1), 105.8(2); C(1)-N(1)-B(1), 127.12(11); C(1A)-N(1)-B(1), 127.12(11); N(1)-B(1)-C(7A), 119.96(12); N(1)-B(1)-C(7), 119.96(12); C(7)-B(1)-C(7A), 120.1(2); C(7)-C(12)-C(15), 122.27(18); C(11)-C(12)-C(15), 117.82(18).

Table S4 Crystallographic experimental details for compound **BCz**.

Empirical formula	$C_{30}H_{30}BN$
Formula weight	415.36
Temperature	296(2) K
Wavelength	0.71073 Å
Crystal system, space group	Monoclinic, C2/c
Unit cell dimensions	a = 12.708(4) Å α = 90 deg.
	b = 10.530 (2) Å β = 90.733(3) deg.
	c = 17.493 (3) Å γ = 90 deg.
Volume	2340.7(11) Å^3
Z, Calculated density	4, 1.179 Mg/m^3
Absorption coefficient	0.067 mm^-1
F(000)	888.0
Crystal size	0.5 x 0.3 x 0.2 mm
Theta range for data collection	4.658 to 51.28 deg.
Limiting indices	-15<=h<=15, -12<=k<=12, -21<=l<=21
Reflections collected / unique	10255 / 2198 [R(int) = 0.0355]
Completeness to theta = 51.28	100 %
Refinement method	Full-matrix least-squares on F^2
Data / restraints / parameters	2198 / 0 / 149
Goodness-of-fit on F^2	1.067
Final R indices [I>2sigma(I)]	R1 = 0.0483, wR2 = 0.1160
R indices (all data)	R1 = 0.0696, wR2 = 0.1332
Extinction coefficient	n/a
Largest diff. peak and hole	0.20 / -0.19 e. Å^-3
CCDC number	1960139

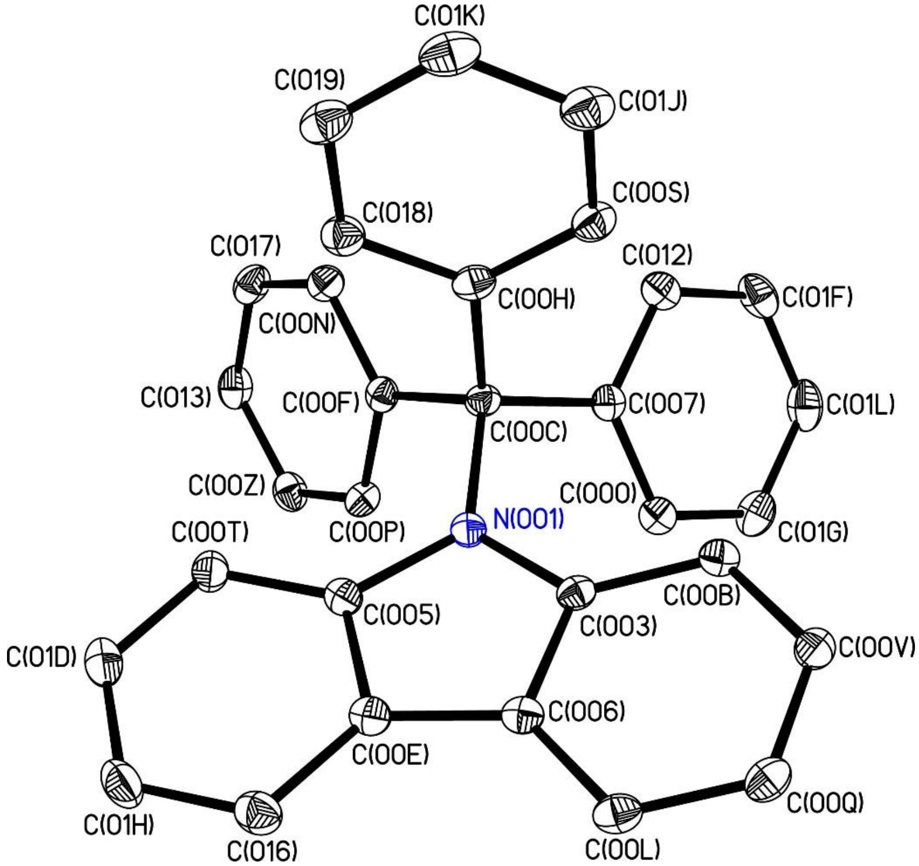

Fig. S27 Molecular Structure of **CCz** with thermal ellipsoids presented at a 50% probability level. All hydrogen atoms have been omitted for clarity. Selected bond lengths (Å): N(001)-C(003), 1.4112(18); N(001)-C(00C), 1.4984(18); N(001)-C(005), 1.4167(18); C(00C)-C(00H), 1.546(2); C(007)-C(00C), 1.546(2); C(00C)-C(00F), 1.549(2). Bond angles (deg): N(001)-C(00C)-C(007), 110.23(11); N(001)-C(00C)-C(00F), 110.32(12); N(001)-C(00C)-C(00H), 105.70(11); C(007)-C(00C)-C(00F), 101.48(12); C(007)-C(00C)-C(00H), 114.51(12); C(00H)-C(00C)-C(00F), 114.66(12).

Table S5 Crystallographic experimental details for compound **CCz**.

Empirical formula	$C_{31}H_{23}N$
Formula weight	409.50
Temperature	150(2) K
Wavelength	0.71073 Å
Crystal system, space group	Triclinic, P-1
Unit cell dimensions	a = 10.109(3) Å α = 74.600(4) deg.
	b = 14.356 (13) Å β = 77.581(4) deg.
	c = 15.707(5) Å γ = 81.407(4) deg.
Volume	2135.9(11) Å^3
Z, Calculated density	4, 1.273 Mg/m^3
Absorption coefficient	0.073 mm^-1
F(000)	864.0
Crystal size	0.4 x 0.3 x 0.1 mm
Theta range for data collection	2.956 to 53.276 deg.
Limiting indices	-12<=h<=12, -17<=k<=17, -19<=l<=19
Reflections collected / unique	23266 / 8829 [R(int) = 0.0412]
Completeness to theta = 53.276	100.0 %
Refinement method	Full-matrix least-squares on F^2
Data / restraints / parameters	8829 / 0 / 761
Goodness-of-fit on F^2	1.004
Final R indices [I>2sigma(I)]	R1 = 0.0425, wR2 = 0.0740
R indices (all data)	R1 = 0.0766, wR2 = 0.0841
Extinction coefficient	n/a
Largest diff. peak and hole	0.22 / -0.17 e. Å^-3
CCDC number	1960144

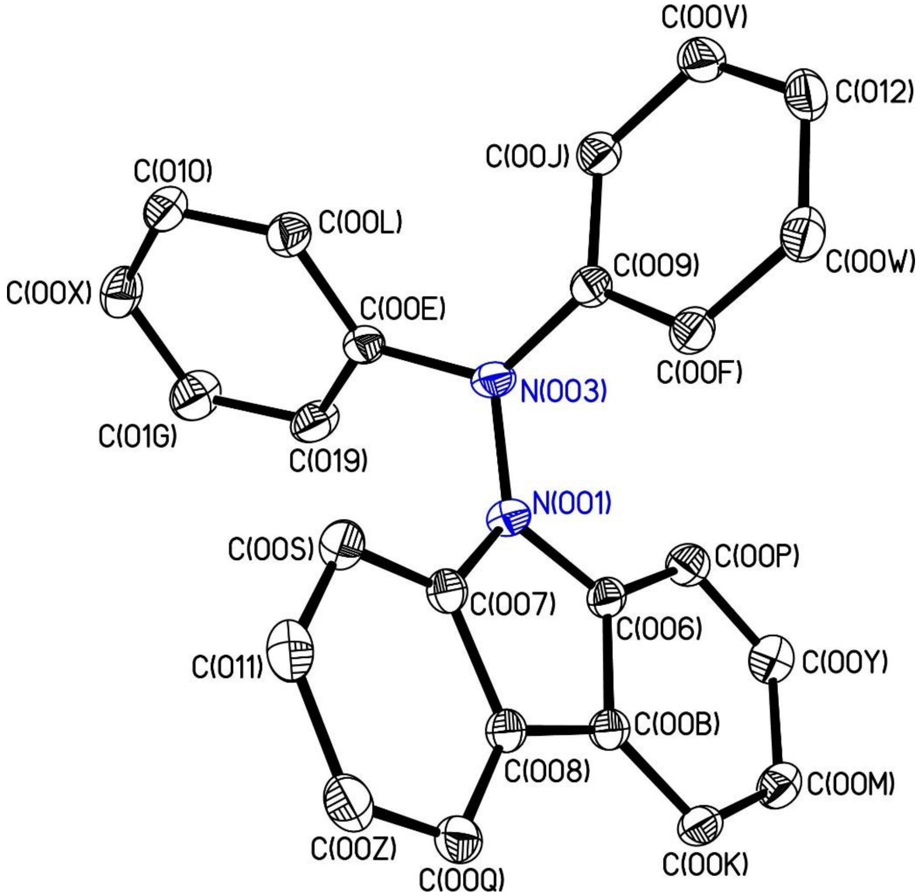

Fig. S28 Molecular Structure of **NCz** with thermal ellipsoids presented at a 50% probability level. All hydrogen atoms have been omitted for clarity. Selected bond lengths (Å): N(001)-N(003), 1.3905(17); N(001)-C(006), 1.393(2); N(001)-C(007), 1.398(2); N(003)-C(009), 1.4200(19); N(003)-C(00E), 1.4331(19); C(008)-C(00B), 1.454(2). Bond angles (deg): N(003)-N(001)-C(006), 123.30(13); N(003)-N(001)-C(007), 125.45(13); C(006)-N(001)-C(007), 109.93(12); N(001)-N(003)-C(009), 116.42(12); N(001)-N(003)-C(00E), 114.65(12); C(009)-N(003)-C(00E), 125.70(12); N(001)-C(006)-C(00B), 107.95(14); C(00P)-C(006)-N(001), 129.51(14); N(001)-C(007)-C(008), 107.79(13); C(00J)-C(009)-N(003), 120.00(14); C(00F)-C(009)-N(003), 120.36(14); C(00S)-C(007)-N(001), 129.64(15); C(00L)-C(00E)-N(003), 121.87(14); C(019)-C(00E)-N(003), 118.53(14).

Table S6 Crystallographic experimental details for compound **NCz**.

Empirical formula	$C_{24}H_{18}N_2$
Formula weight	334.40
Temperature	150(2) K
Wavelength	0.71073 (Å)
Crystal system, space group	Monoclinic, P21/n
Unit cell dimensions	a = 17.468(3) Å α = 90 deg. b = 11.603(2) Å β = 113.128(2) deg. c = 18.830(3) Å γ = 90 deg.
Volume	3509.6(11) Å^3
Z, Calculated density	8, 1.266 Mg/m^3
Absorption coefficient	0.074 mm^-1
F(000)	1408.0
Crystal size	0.6 x 0.3 x 0.2 mm
Theta range for data collection	4.08 to 53.41 deg.
Limiting indices	-21<=h<=22, -14<=k<=14, -23<=l<=23
Reflections collected / unique	37109 / 7377 [R(int) = 0.0392]
Completeness to theta = 53.41	100.0%
Refinement method	Full-matrix least-squares on F^2
Data / restraints / parameters	7377 / 0 / 613
Goodness-of-fit on F^2	1.011
Final R indices [I>2sigma(I)]	R1 = 0.0412, wR2 = 0.0885
R indices (all data)	R1 = 0.0674, wR2 = 0.1008
Extinction coefficient	n/a
Largest diff. peak and hole	0.29 / -0.17 e. Å^-3
CCDC number	1960140

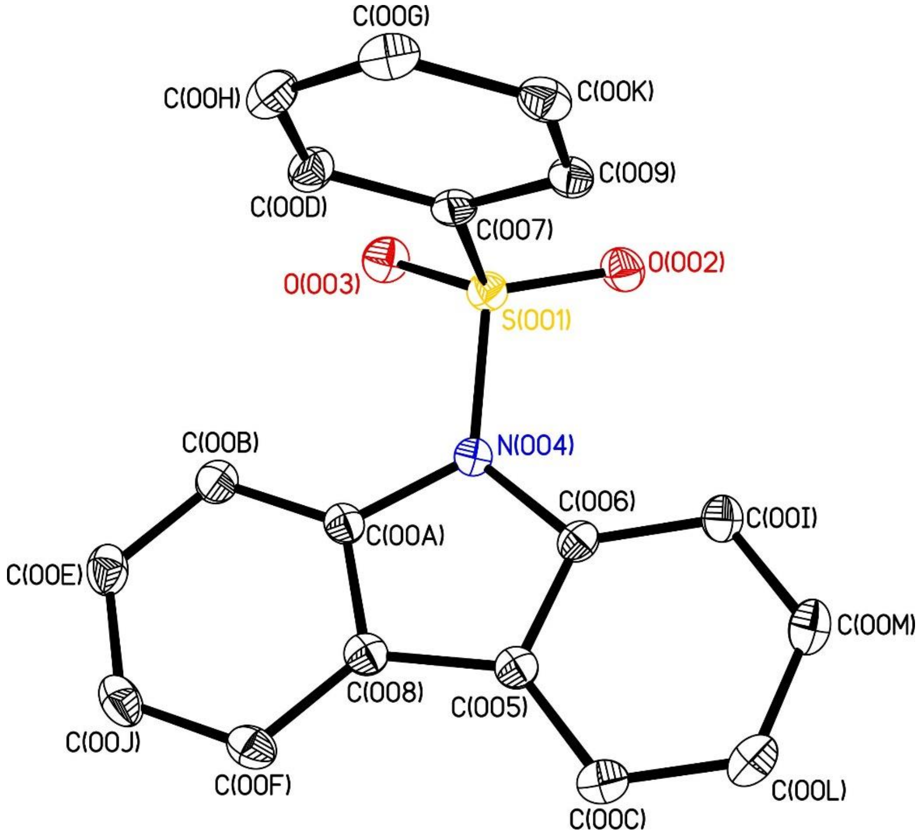

Fig. S29 Molecular Structure of **SOCz** with thermal ellipsoids presented at a 50% probability level. All hydrogen atoms have been omitted for clarity. Selected bond lengths (Å): S(001)-O(002), 1.4307(12); S(001)-O(003), 1.4295(12); S(001)-N(004), 1.6676(14); S(001)-C(007), 1.7645(16); N(004)-C(00A), 1.4392(19); C(005)-C(008), 1.455(2). Bond angles (deg): O(002)-S(001)-N(004), 106.24(7); O(002)-S(001)-C(007), 109.12(7); O(003)-S(001)-O(002), 120.02(7); O(003)-S(001)-N(004), 106.59(7); O(003)-S(001)-C(007), 109.38(8); N(004)-S(001)-C(007), 104.30(7); C(006)-N(004)-S(001), 123.70(11); C(00A)-N(004)-S(001), 122.90(11); C(005)-C(006)-N(004), 108.36(13); C(00I)-C(006)-N(004), 130.09(15); C(009)-C(007)-S(001), 119.35(12); C(00D)-C(007)-S(001) 118.90(12); C(008)-C(00A)-N(004), 108.23(13); C(00B)-C(00A)-N(004), 129.72(15).

Table S7 Crystallographic experimental details for compound **SOCz**.

Empirical formula	$C_{18}H_{13}NO_2S$
Formula weight	307.35
Temperature	150(2) K
Wavelength	0.71073 (Å)
Crystal system, space group	Monoclinic, C2/c
Unit cell dimensions	a = 22.383(5) Å α = 90 deg.
	b = 10.788(2) Å β = 124.535(2) deg.
	c = 14.435(3) Å γ = 90 deg.
Volume	2871.4(11) Å^3
Z, Calculated density	8, 1.422 Mg/m^3
Absorption coefficient	0.232 mm^-1
F(000)	1280.0
Crystal size	0.4 x 0.3 x 0.2 mm
Theta range for data collection	4.374 to 53.418 deg.
Limiting indices	-28<=h<=28, -13<=k<=13, -18<=l<=18
Reflections collected / unique	13883 / 3021 [R(int) = 0.0312]
Completeness to theta = 53.418	100.0%
Refinement method	Full-matrix least-squares on F^2
Data / restraints / parameters	3021 / 0 / 251
Goodness-of-fit on F^2	1.039
Final R indices [I>2sigma(I)]	R1 = 0.0337, wR2 = 0.0815
R indices (all data)	R1 = 0.0439, wR2 = 0.0873
Extinction coefficient	n/a
Largest diff. peak and hole	0.36 and -0.33 e. Å^-3
CCDC number	1960141

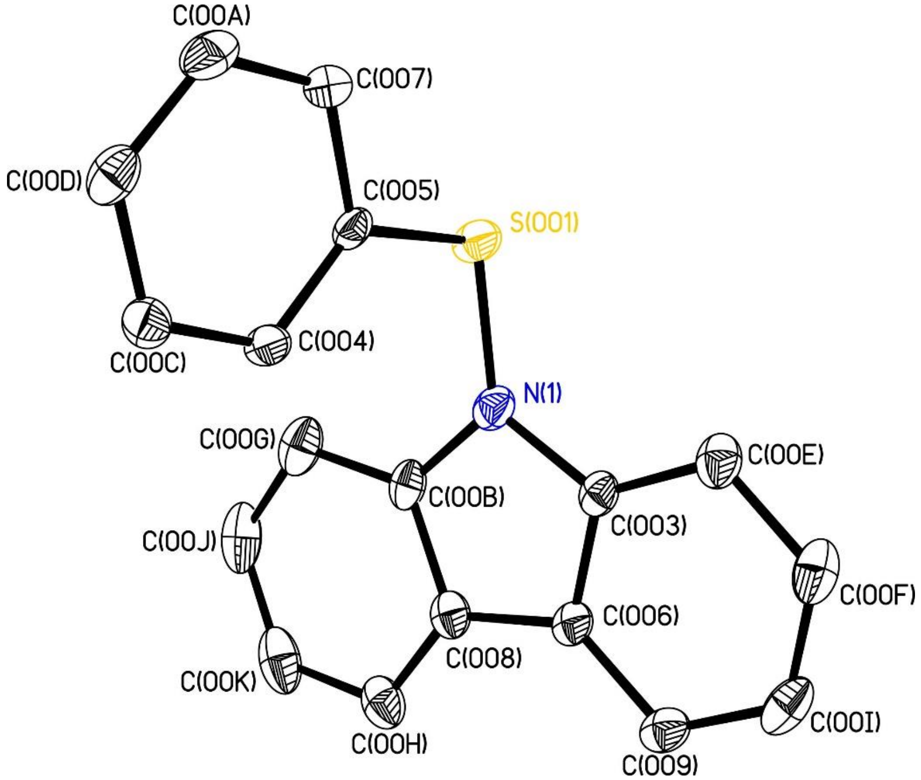

Fig. S30 Molecular Structure of **SCz** with thermal ellipsoids presented at a 50% probability level. All hydrogen atoms have been omitted for clarity. Selected bond lengths (Å): S(001)-N(1), 1.680(3); S(001)-C(005), 1.771(3); N(1)-C(003), 1.410(4); N(1)-C(00B), 1.407(4); C(006)-C(008), 1.454(5); C(00B)-C(00G), 1.394(5); C(003)-C(00E), 1.389(5). Bond angles (deg): N(1)-S(001)-C(005), 103.63(14); C(003)-N(1)-S(001), 125.3(2); C(00B)-N(1)-S(001), 126.4(2); C(00B)-N(1)-C(003), 108.2(3); C(006)-C(003)-N(1), 108.6(3); C(00E)-C(003)-N(1), 128.8(3); C(004)-C(005)-S(001), 124.4(2); C(007)-C(005)-S(001), 115.7(2).

Table S8 Crystallographic experimental details for compound **SCz**.

Empirical formula	$C_{19}H_{13}S$
Formula weight	273.35
Temperature	296.15 K
Wavelength	0.71073 (Å)
Crystal system, space group	Orthorhombic, P212121
Unit cell dimensions	a = 5.737(2) Å α = 90 deg.
	b = 8.119(3) Å β = 90 deg.
	c = 29.889(10) Å γ = 90 deg.
Volume	1392.2(8) Å^3
Z, Calculated density	4, 1.314 Mg/m^3
Absorption coefficient	0.220 mm^-1
F(000)	576.0
Crystal size	0.5 x 0.3 x 0.2 mm
Theta range for data collection	2.726 to 51.896 deg.
Limiting indices	-7<=h<=6, -9<=k<=9, -36<=l<=36
Reflections collected / unique	12872 / 2677 [R(int) = 0.0341]
Completeness to theta = 51.896	100.0%
Refinement method	Full-matrix least-squares on F^2
Data / restraints / parameters	2677 / 0 / 181
Goodness-of-fit on F^2	1.125
Final R indices [I>2sigma(I)]	R1 = 0.0363, wR2 = 0.0832
R indices (all data)	R1 = 0.0432, wR2 = 0.0882
Extinction coefficient	n/a
Largest diff. peak and hole	0.30 and -0.18 e. Å^-3
CCDC number	1960142

10. Intermolecular interactions of XCz (X = B, C, N, S) in crystal

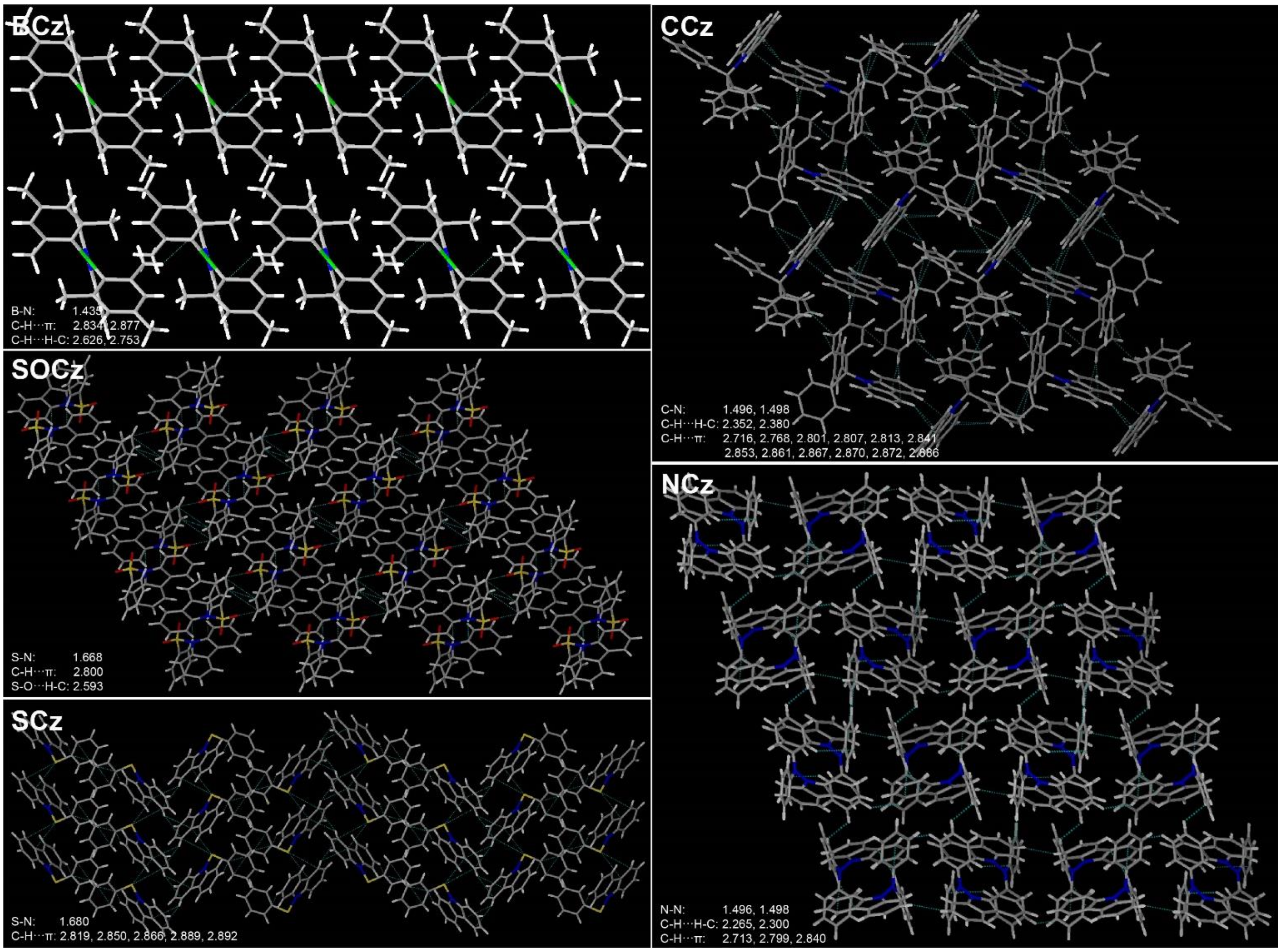

Fig. S31 Single-crystal structure and molecular packing of **XCz** with denoted intermolecular interactions.

The crystal packing of **XCz** indicated that the network was constructed by C-H···π, π···π, and C-H···H-C bonding interactions. These hydrogen bonds provide stabilizing energy for crystal packing and confine molecular geometry, thus, the molecular movement will be largely restricted in the photophysical process between the ground and excited states.

11. Computational methods and results

The quantum mechanics/molecular mechanics (QM/MM) theory with two-layer ONIOM method was implemented to deal with the electronic structures in crystal, where the central molecule is chosen as the active QM part and set as the high layer, while the surrounding ones are chosen as the MM part and defined as the low layer. The universal force field (UFF) was used for the MM part, and the molecules of MM part were frozen during the QM/MM geometry optimizations. The electronic embedding is adopted in QM/MM calculations by incorporating the partial charges of the MM region into the quantum mechanical Hamiltonian. The (U)B3LYP functional was used to optimized the lowest triplet states (T_1), together with a 6-31G(d) basis set for the remaining atoms. The vertical excitation energies and natural transition orbitals (NTOs) for the low-lying excited states were evaluated by TDDFT/B3LYP/6-31G(d)//PBE method using Gaussian 09 package.[6] At the same level, the spin-orbit couplings between singlet ant triplet states were calculated by ORCA computational chemistry package.[7, 8]

Mulliken charge distribution:

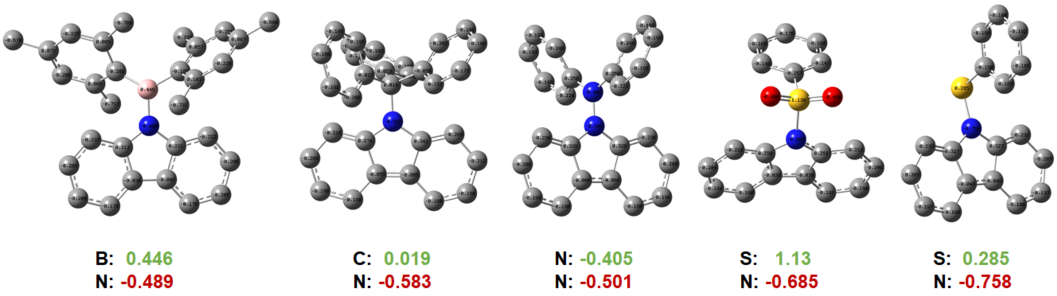

Electronic redistribution resulting from Lewis acid–base complexation:

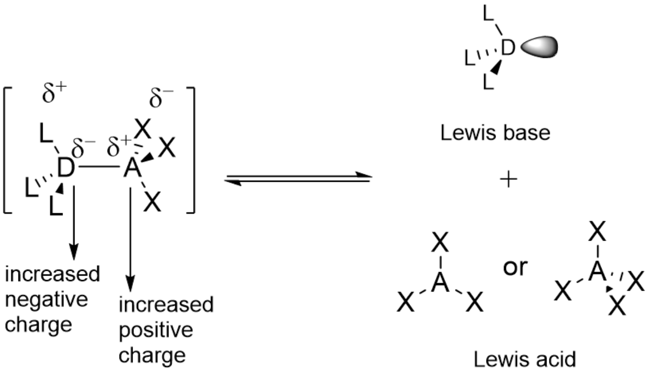

The charge distribution of nitrogen atoms in carbazole plane were larger than the connecting main-group element. Acording to the literature,[9] this result suggesting the donor is carbazole and the accepter is main-group units.

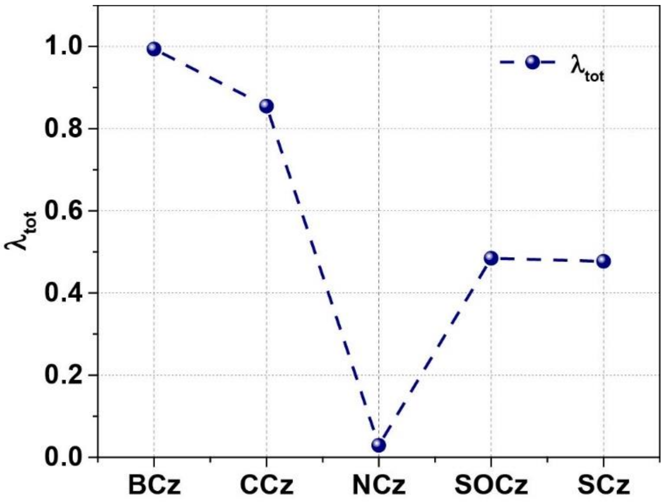

Fig. S32 The reorganization energy (λ_{tot}) of **XCz** between S_0 and T_1.

12. The detailed data for *in vivo* experiments

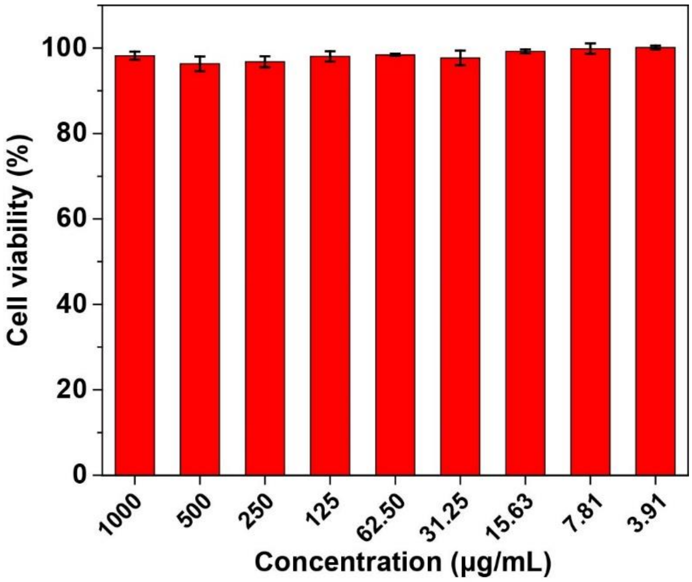

Fig. S33 Viability of cells after incubation with different concentrations of **CCz**-Cm nanoparticles for 48 h. The error bars represent the standard deviations of three parallel measurements.

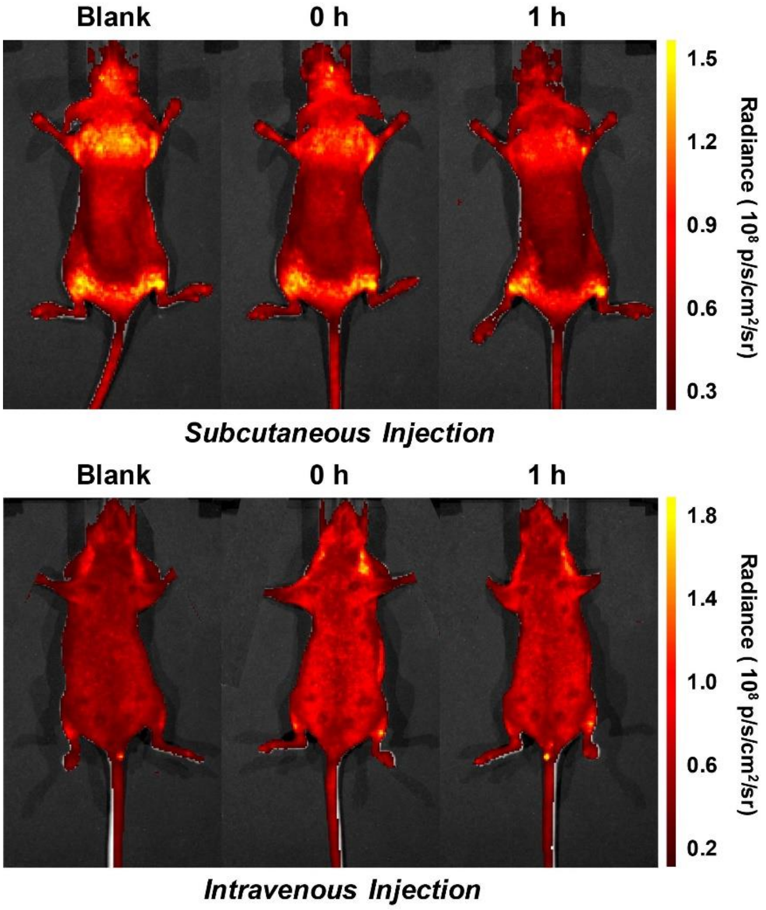

Fig. S34 Fluorescence imaging of mice injected with **CCz**-Cm nanoparticles at different time points (0, 1h).

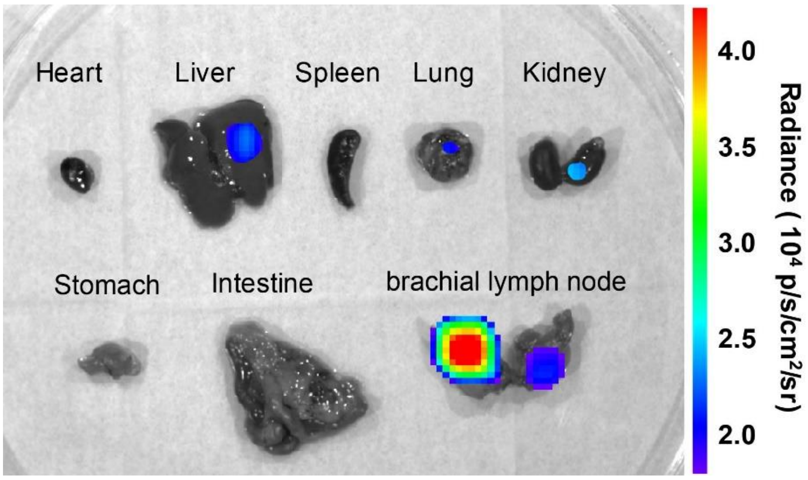

Fig. S35 Afterglow imaging of major organs and brachial lymph node after tail intravenous injected with **CCz**-Cm nanoparticles.

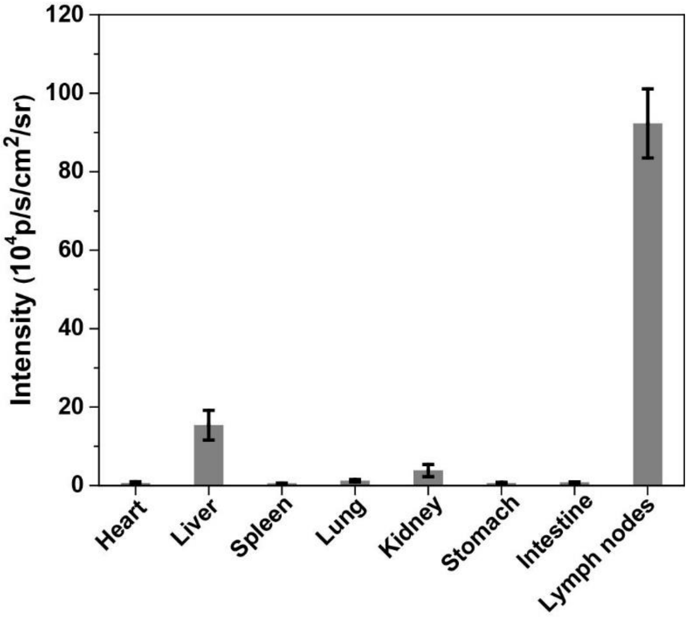

Fig. S36 UOP intensity for **CCz**-Cm nanoparticles on major organs and brachial lymph node of mice. The error bars represent the standard deviations of three parallel measurements.

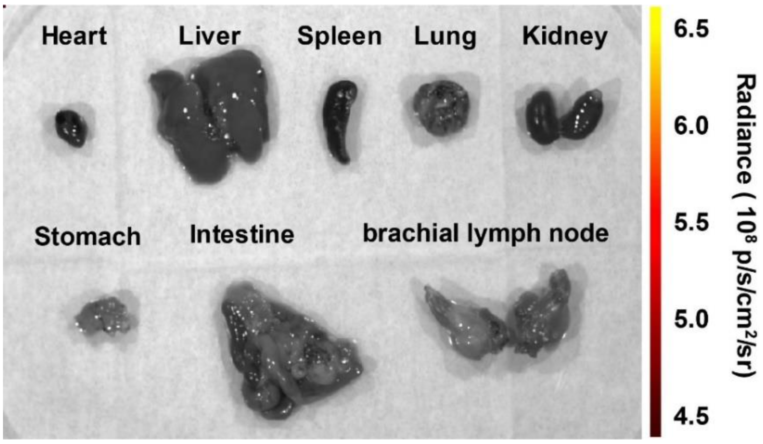

Fig. S37 Fluorescence imaging of major organs and brachial lymph node after tail intravenous injected with **CCz**-Cm nanoparticles.

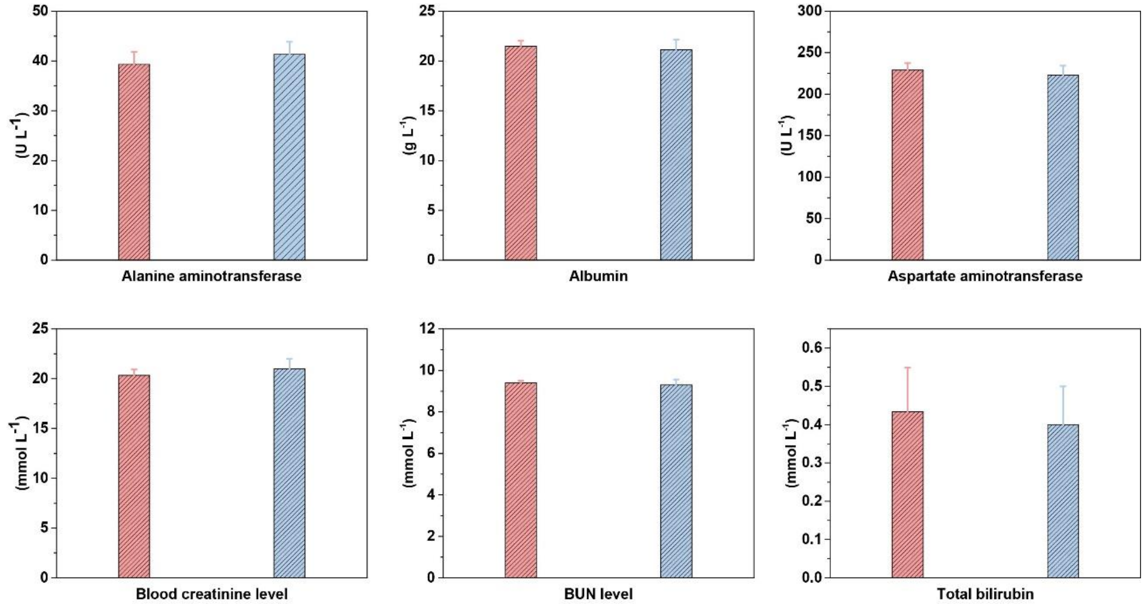

Fig. S38 Blood test parameters regarding the mice liver and kidney function with and without loaded **CCz**-Cm nanoparticles. The error bars represent the standard deviations of three parallel measurements.

13. The ^{1}H and ^{13}C NMR spectra of XCz in $CDCl_3$

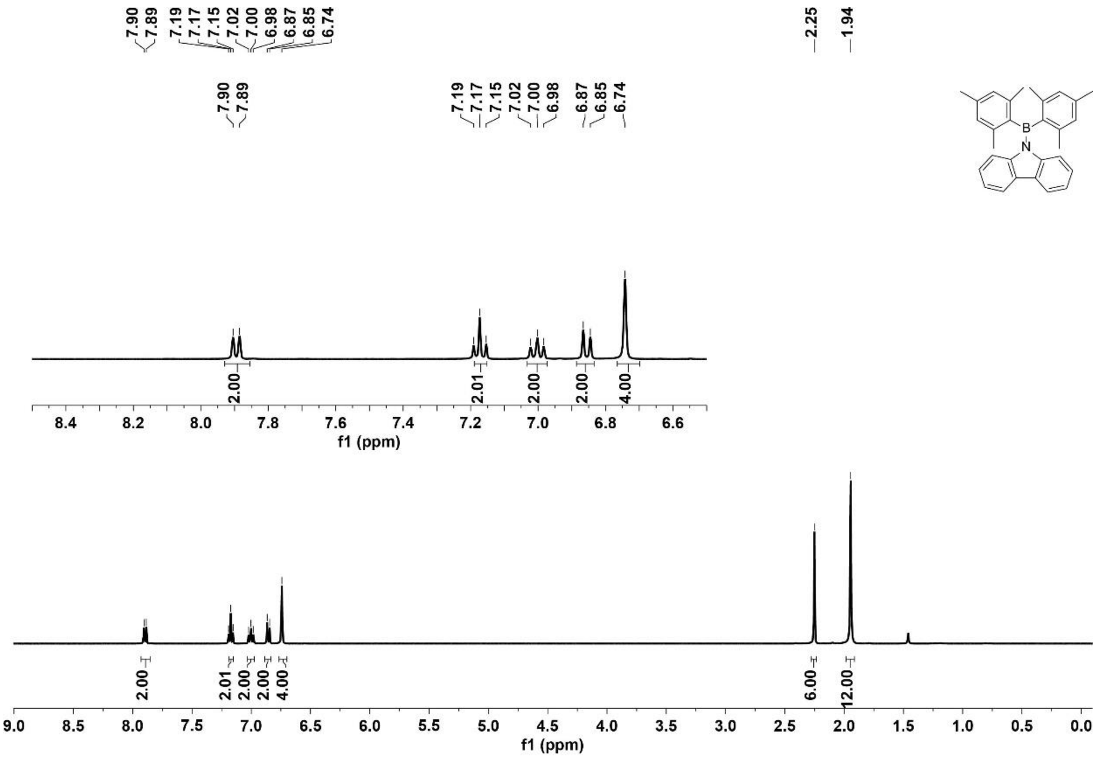

Fig. S39 The ^{1}H NMR spectrum of **BCz** in $CDCl_3$.

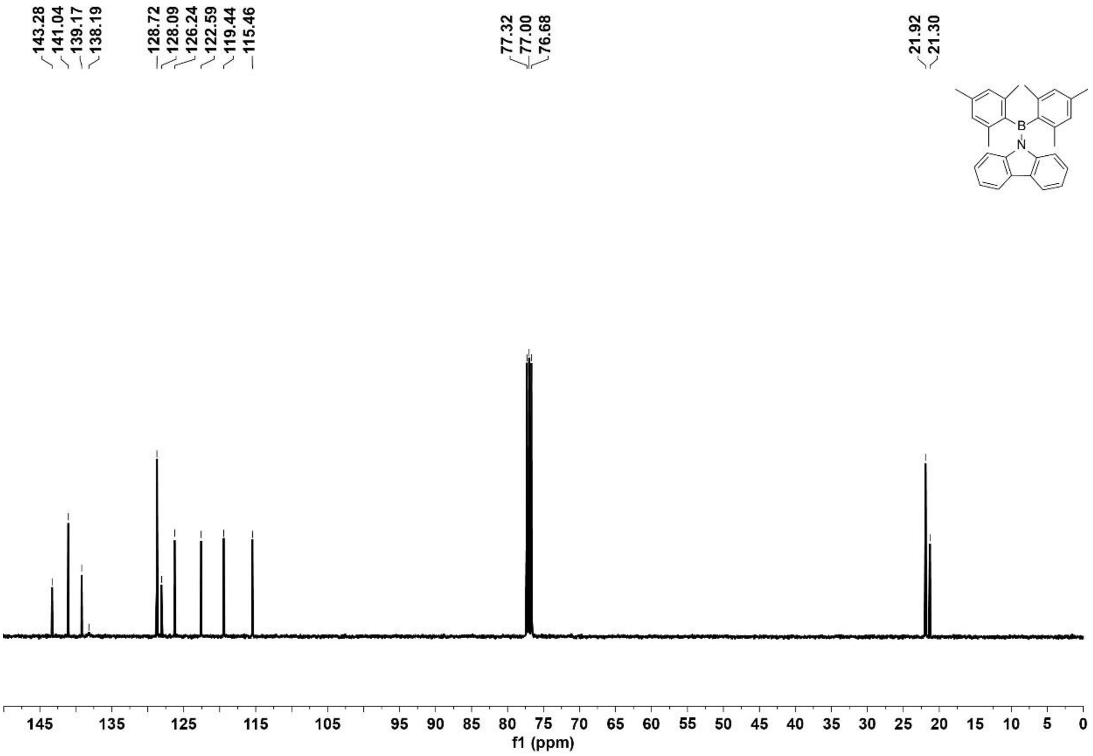

Fig. S40 The ^{13}C NMR spectrum of **BCz** in $CDCl_3$.

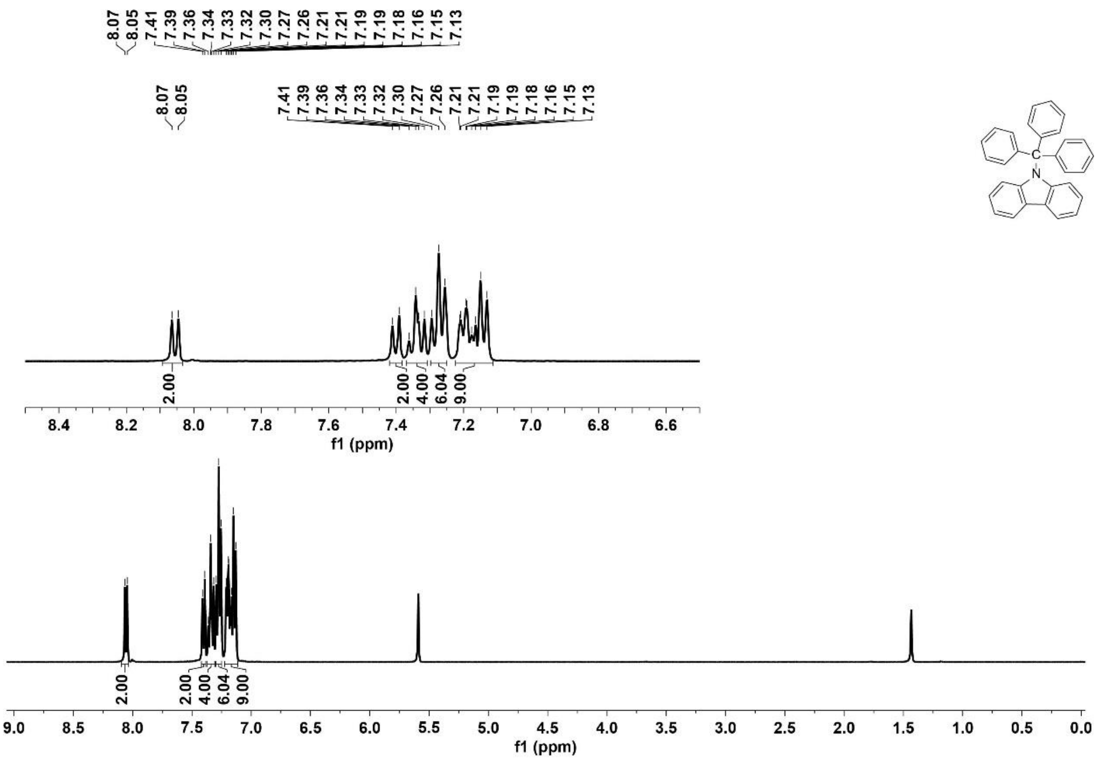

Fig. S41 The ^{1}H NMR spectrum of **CCz** in $CDCl_3$.

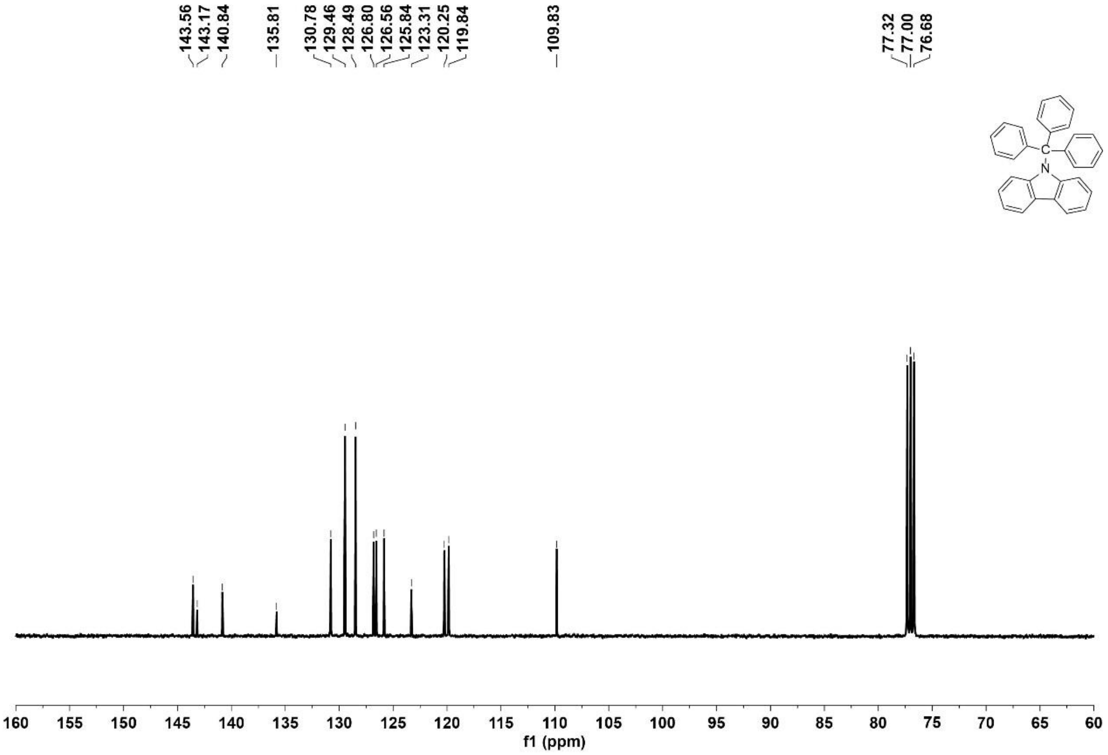

Fig. S42 The ^{13}C NMR spectrum of **CCz** in $CDCl_3$.

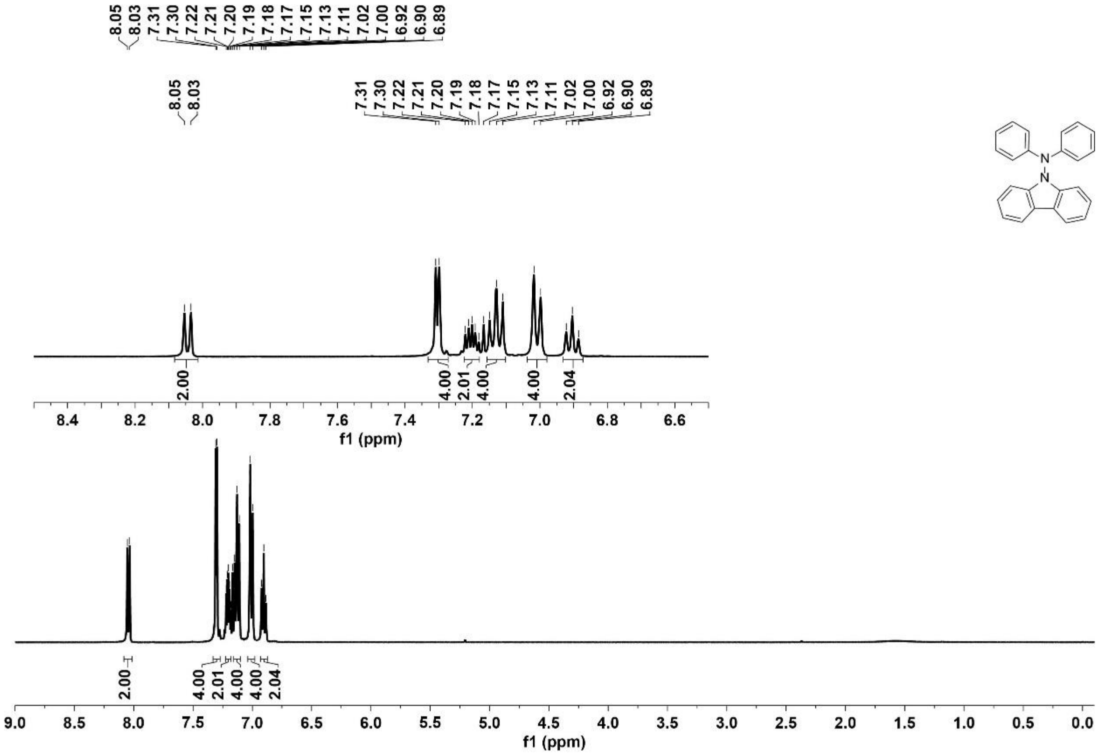

Fig. S43 The ^{1}H NMR spectrum of **NCz** in CDCl$_3$.

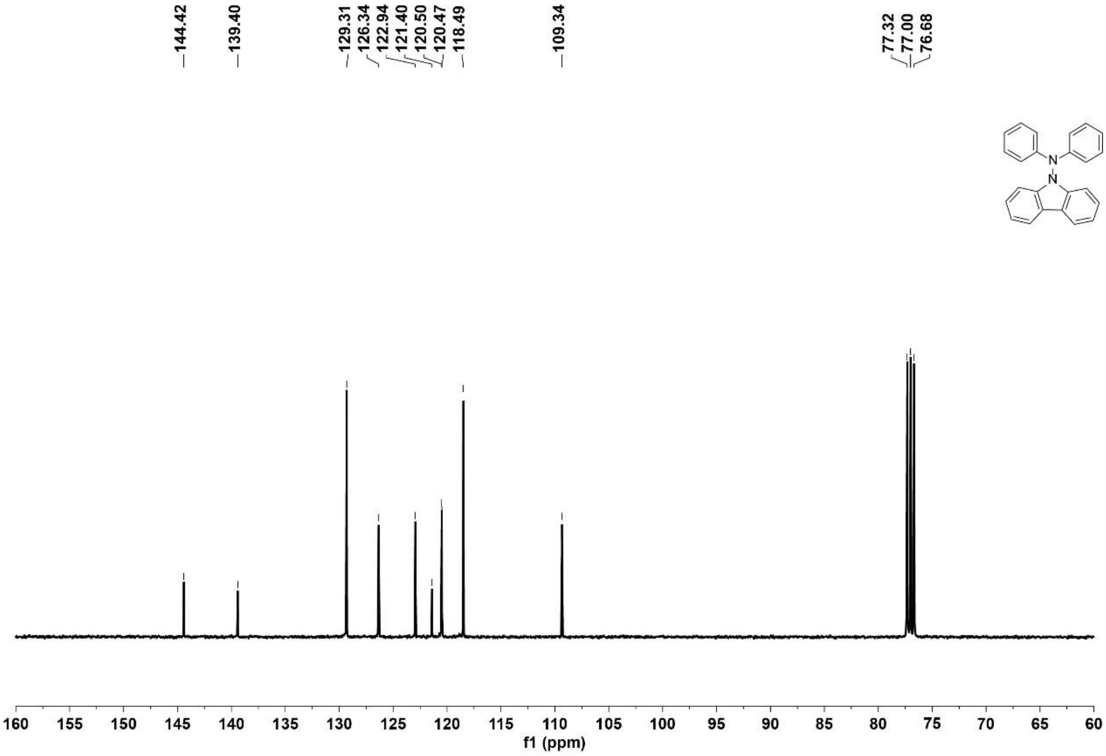

Fig. S44 The ^{13}C NMR spectrum of **NCz** in CDCl$_3$.

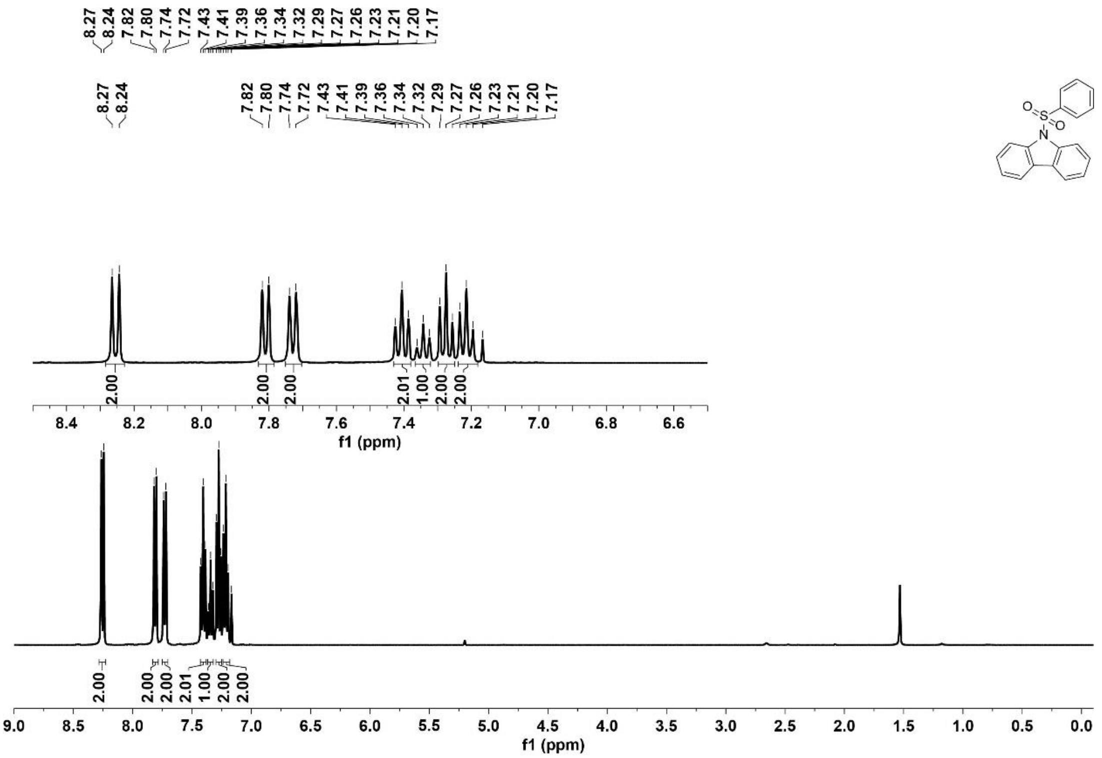

Fig. S45 The ^{1}H NMR spectrum of **SOCz** in CDCl$_3$.

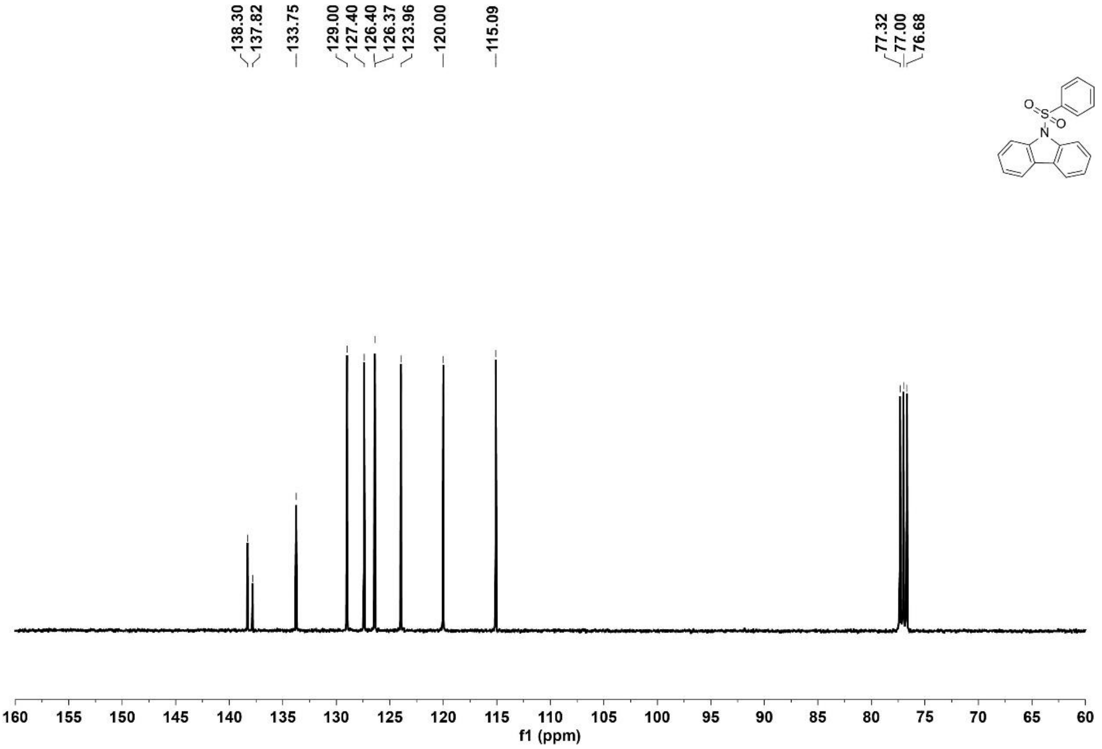

Fig. S46 The ^{13}C NMR spectrum of **SOCz** in CDCl$_3$.

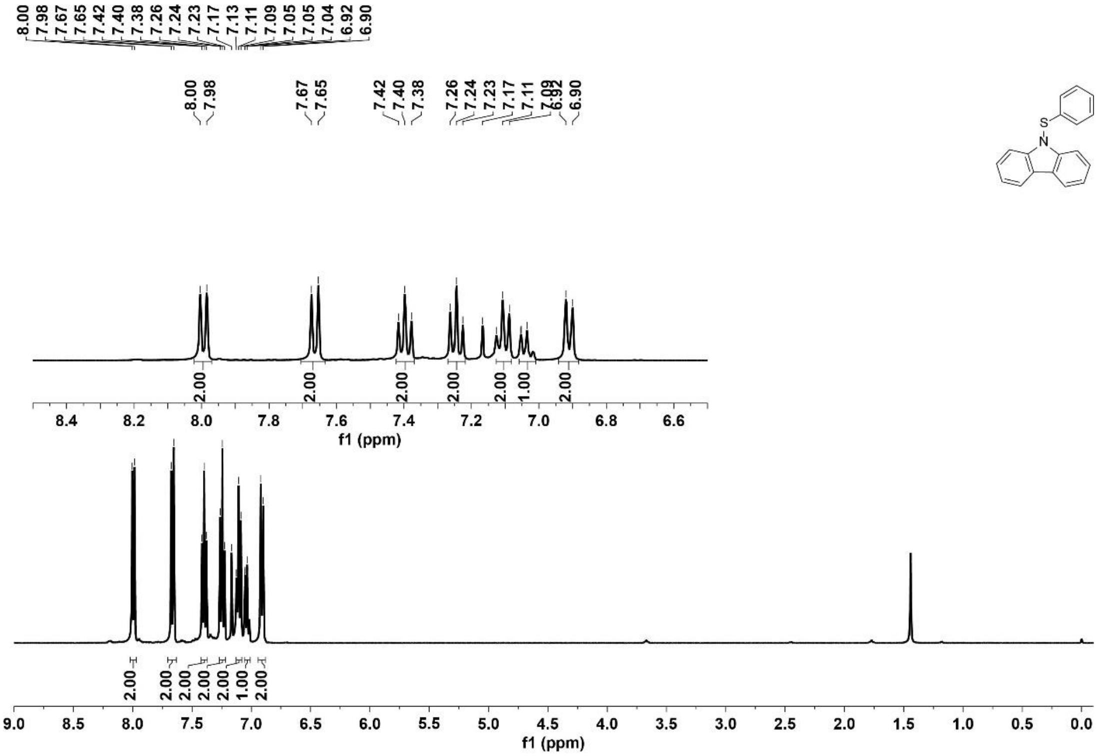

Fig. S47 The ^{1}H NMR spectrum of **SCz** in $CDCl_3$.

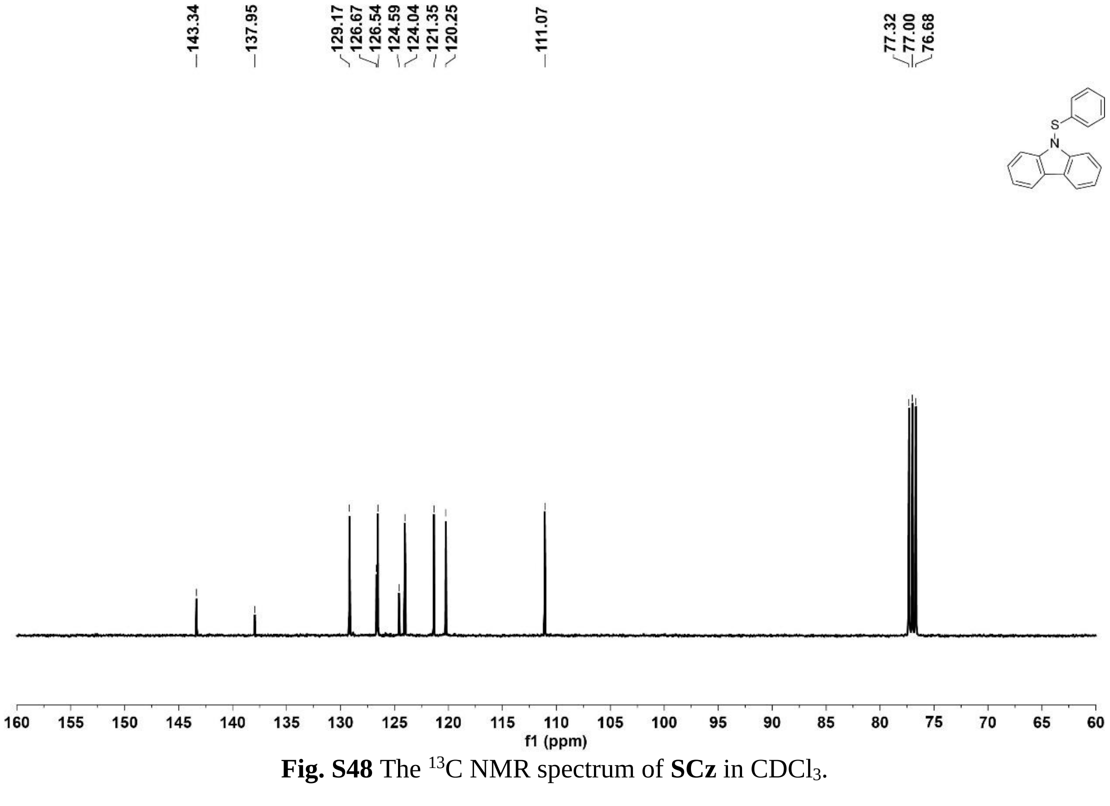

Fig. S48 The ^{13}C NMR spectrum of **SCz** in $CDCl_3$.

Reference

1. L. C. Campeau, M. Parisien, A. Jean and K. Fagnou, *J. Am. Chem. Soc.*, 2006, **128**, 581-590.
2. M. H. Ali and S. L. Buchwald, *J. Org. Chem.*, 2001, **66**, 2560-2565.
3. S. Cai, H. Shi, J. Li, L. Gu, Y. Ni, Z. Cheng, S. Wang, W. W. Xiong, L. Li, Z. An and W. Huang, *Adv. Mater.*, 2017, **29**, 1701244.
4. Z. He, H. Gao, S. Zhang, S. Zheng, Y. Wang, Z. Zhao, D. Ding, B. Yang, Y. Zhang and W. Z. Yuan, *Adv. Mater.*, 2019, **31**, e1807222.
5. X. Zhen, Y. Tao, Z. An, P. Chen, C. Xu, R. Chen, W. Huang and K. Pu, *Adv. Mater.*, 2017, **29**, 1606665.
6. M. Frisch, G. Trucks, H. B. Schlegel, G. Scuseria, M. Robb, J. Cheeseman, G. Scalmani, V. Barone, B. Mennucci and G. Petersson, *Inc., Wallingford, CT*, 2009, **200**.
7. F. Neese, *Wiley Interdiscip. Rev. Comput. Mol. Sci.*, 2012, **2**, 73-78.
8. F. Neese, *Wiley Interdiscip. Rev. Comput. Mol. Sci.*, 2018, **8**, e1327.
9. S. E. Denmark and G. L. Beutner, *Angew. Chem., Int. Ed.*, 2008, **47**, 1560-1638.